Supporting Information for

Landscape of somatic mutations and clonal evolution in mantle cell lymphoma

Sílvia Beà[1], Rafael Valdés-Mas[2], Alba Navarro[1], Itziar Salaverria[1], David Martín-Garcia[1], Pedro Jares[1,3], Eva Giné[4], Magda Pinyol[5], Cristina Royo[1], Ferran Nadeu[1], Laura Conde[1], Manel Juan[6], Guillem Clot[1], Pedro Vizán[7], Luciano Di Croce[7], Diana A. Puente[2], Mónica López-Guerra[1], Alexandra Moros[1], Gael Roue[1], Marta Aymerich[1], Neus Villamor[1], Lluís Colomo[1,3], Antonio Martínez[1,3], Alexandra Valera[1], José I. Martín-Subero[1,3], Virginia Amador[1], Luis Hernández[1], Maria Rozman[1], Anna Enjuanes[5], Pilar Forcada[8], Ana Muntañola[8], Elena M. Hartmann[9], María J. Calasanz[10], Andreas Rosenwald[9], German Ott[11], Jesús M. Hernández-Rivas[12], Wolfram Klapper[13], Reiner Siebert[14], Adrian Wiestner[15], Wyndham H. Wilson[16], Dolors Colomer[1], Armando López-Guillermo[4], Carlos López-Otín[2]*, Xose S. Puente[2]* & Elías Campo[1,3]*

To whom correspondence should be addressed: SBEA@clinic.ub.es (S.B.), xspuente@uniovi.es (X.S.P.) and ECAMPO@clinic.ub.es (E.C.)

Contents of this PDF file:

SI Materials and Methods

Patients and samples. We studied 29 patients with mantle cell lymphoma (MCL) (1), who had given informed consent in agreement with the Institutional Review Board of Hospital Clínic (Barcelona, Spain) for sample collection and analysis following the guidelines of the International Cancer Genome Consortium (2). Informed consent to participate in the study was obtained according to the guidelines of the local Ethic Committees. Four patients were selected for whole-genome sequencing (WGS) and all 29 cases were studied by whole-exome sequencing (WES). Clinical and biological characteristics of these patients are summarized in Tables S1-S3. Twenty-six tumors were studied at diagnosis or previous to treatment and three at relapse. Additional independent tumor samples of eight patients were analyzed by WGS (n=2) or WES (n=8). Six of them were obtained synchronically from two different topographic sites whereas in two patients the samples were obtained sequentially at two different time points (Table S1). Constitutional DNA was obtained from normal peripheral blood in all patients. Additionally, six well characterized MCL cell lines were analyzed by WES (Table S4). An additional cohort of 172 MCL patients and 3 MCL cell lines were used for clinical and mutational validation of selected genes (Table S3-S4). The study was approved by the Institutional Review Board of Hospital Clínic (Barcelona, Spain).

For WES analysis, a total of 37 tumor samples were obtained from PB (n=22), lymph nodes (n=12), or other involved tissues (tonsil, spleen, colon, n=3). Peripheral blood tumor cells were purified using an immunomagnetic method previously described (3, 4). Tumor cell purity was ≥80% as assessed by flow cytometry. Normal cells were purified from blood in all patients and had no detectable or less than 4% tumor cells also assessed by flow cytometry. Tumor DNA was extracted using appropriate Qiagen kits (Qiagen) as previously described (5).

Rainfall plots and *Kataegis.* Rainfall plots based on WGS data were constructed by computing the distance between one somatic mutation to the previous one (6). *Kataegis* in MCL was defined as regions containing at least five independent somatic mutations in less than 1 Kb. Rainfalls were considered when there was a cluster of proximal mutations between 1 and 10,000 bases ($\log_{10}$ distance between 0-4).

Clonal evolution analyses. To identify the subclonal architectural evolution from WES data, the frequency of reads supporting the mutated allele was calculated for each somatic substitution. Only positions with a minimum depth of coverage of 20, and not present in regions of copy number alterations (CNA) were considered for clustering analysis. Three different clusters of mutations were considered: i) shared and stable mutations among both samples; ii) mutations specific of the first sample; and iii) mutations identified only in the second sample. All mutations were used to compute the clusters but only the protein-coding mutations were used for graphical representation of the results.

***IGHV* mutational status and *SOX11* expression.** *IGHV-IGHD-IGHJ* rearrangements and mutational status were analyzed using leader or consensus primers for the *IGHV* FR1 along with appropriate consensus primers, as previously described (5). Sequences with ≥97% identity to the germ line were considered unmutated (5, 7). *SOX11* expression was evaluated either by quantitative RT-PCR or immunohistochemistry and categorized as positive or negative as previously described (5).

Sanger sequencing validation. *TP53, WHSC1, BIRC3, NOTCH2, NOTCH1, MEF2B, TLR2* and *B2M* genes were investigated in an expanded cohort of patients by PCR followed by direct Sanger sequencing. Oligonucleotide primers for PCR amplification were designed using Primer 3. Primers used are specified in Table S13. Sequences were analyzed with the Mutation Surveyor® (Softgenetics).

SNP-arrays. Samples were genotyped using Affymetrix SNP6.0 microarrays (Affymetrix) according to the manufacturer's instructions as previously described (5). Copy number data from SNP6.0 were visualized and analyzed using Nexus CN 6.0 Discovery Edition (Biodiscovery). All alterations were visually inspected by two different observers (I.S. and S.B). Alterations were cross-checked in the copy number variation database (http://projects.tcag.ca/variation/). Copy number neutral-loss of heterozygosity (CNN-LOH) was considered when the size of the altered region was >5Mb. According to the literature, cases were considered to have chromothripsis when at least ten switches between two or more copy number states were apparent on an individual chromosome (8). CNA were also analyzed from WES data with a method previously described (9) and compared to SNP-array data.

Gene expression profiling. Total RNA was extracted with the TRIzol reagent following the recommendations of the manufacturer (Life Technologies). RNA integrity was examined with the Agilent 2100 Bioanalyzer (Agilent Technologies) and only high quality RNA samples were hybridized to Gene Chip Human Genome U133 plus 2.0 arrays, according to Affymetrix standard protocols. The analysis of the scanned images and the determination of the detection call for each probe set of the array were obtained with the Affymetrix Genechip Command Console. Summarized expression values were computed using the robust multichip average approach implemented in the Expression Console Software (Affymetrix). Differential expression analysis among *WHSC1* and *NOTCH2* -mutated and -unmutated MCL was performed by a multivariate permutation test implemented in the BRB-tool application. We used the multivariate permutation test to provide 90% confidence that the false discovery rate was less than 5%. Enrichment pathway analysis was performed using the GSEA desktop application (GSEA, Broad Institute at MIT:

http://www.broadinstitute.org/gsea/) with MCL tumors with or without mutations in *WHSC1* or *NOTCH2* genes.

TLR stimulation assay. TLR stimulation assays were performed using tumor cells from two patients, MCL patient M021 and a chronic lymphocytic leukemia (CLL) previously published (3) with the *TLR2* mutation p.D327V, one MCL patient with the p.Y298S mutation, four MCL and three CLL patients with wild type *TLR2*, and purified B-lymphocytes from four healthy donors. Samples were cultured in X-Vivo™ 15 medium (Lonza) supplemented with 10% human AB serum (Sigma GmbH) for 48 hours with several TLR2 agonists (Invivogen) following concentrations suggested by the manufacturer or IL-1beta as control. Samples were then assessed for response of 25 cytokines (IL-1β, IL-1RA, IL-2, IL-2R, IL-4, IL-5, IL-6, IL-7, IL-10, IL-12 (p40), IL-13, IL-15, IL-17, TNF-α, IFN-α, IFN-γ, GM-CSF, MIG, CXCL8/IL-8, CXCL10/IP-10, CCL2/MCP-1 CCL3/MIP-1α, CCL4/MIP-1β, CCL5/RANTES and CCL11/Eotaxin). Cells were first incubated with 10 μg/mL of polymyxin B (Sigma, P-4932) for 20 min except in LPS-incubated samples. *In vitro* cytokine production was initially assessed in cell culture supernatants using fluorescence-activated cell sorter analysis (Luminex100 System). Cytokine Human 25-plex panel (Invitrogen), a multiplexed sandwich immunoassays based on flow cytometry Luminex technology, was used to measure the 25 cytokines of the kit. Net median fluorescence intensity data of each cytokine was analyzed with Xponent™ (Luminex) software and results were extrapolated from curves defined by a prequantified standard reagent. Secretion of cytokines was referred to the level of basal secretion without stimulus. All samples were analyzed in duplicate.

For differential TLR2 stimulation assay, we tested Pam3CSK4 1 μg/mL (stimulating TLR1 & 2), FSL-1 1 μg/mL (stimulating TLR2 & 6), HKLM 10^8 cells/mL (TLR2), LPS-PG 10 μg/mL (TLR2), LTA-SA 1 μg/mL (TLR2) and PGN-SA 10 μg/mL (TLR2).

Statistical methods. The PASW Statistics 18.0 (SPSS inc.) and R packages were employed to correlate clinical and biological variables. The independence between categorical clinical parameters and the MCL subgroups was evaluated using Fisher's exact test and continuous variables were compared by Mann-Whitney test. The Wilcoxon rank sum test was used for the comparison of induction levels of interleukin secretion after *TLR2* stimulation in respect to basal secretion levels. Overall survival was measured from date of DNA sampling to date of death or last follow-up, whereas for the allotransplanted patients it was considered until the date of allotransplant. Patients with only available post-treatment DNA were not considered for the survival analysis. Survival curves were plotted according to the Kaplan and Meier method and compared using the log-rank test. Multivariate analysis was performed with the stepwise proportional hazards model (Cox model) assessing that the covariates used in the model and did not violate the proportional hazard assumption. All statistical tests were two-sided and the level of statistical significance was 0.05.

SUPPLEMENTARY FIGURES

Fig. S1 *(A)* Total number of somatic mutations and indels per genome in the four MCL cases (six samples) analyzed by WGS. Tier 1 includes all non-synonymous mutations, coding frameshifts and mutations affecting canonical splicing sites, Tier 2 includes synonymous mutations and mutations in UTRs, and Tier 3 includes the rest of mutations. *(B)* Frequency of substitutions in each sample for the six possible classes of mutation. *The progressed sample M003-PB obtained at progression (3.5 years) showed an increase in the number of mutations. M001, M002: SOX11-positive/*IGHV*-unmutated and M003, M004: SOX11-negative/*IGHV*-mutated.

A

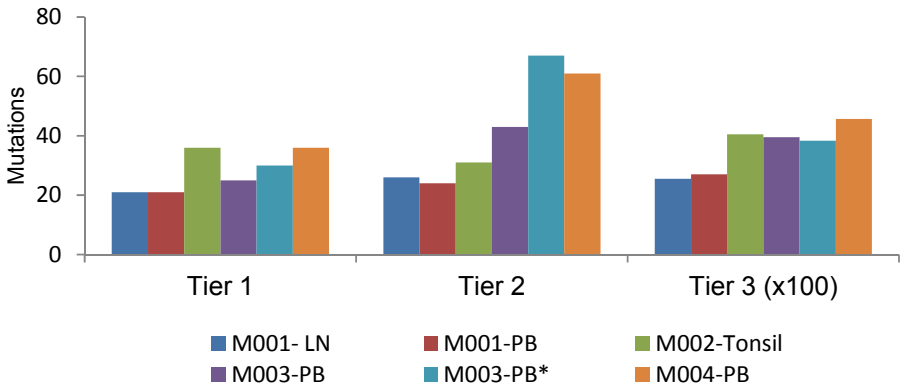

B

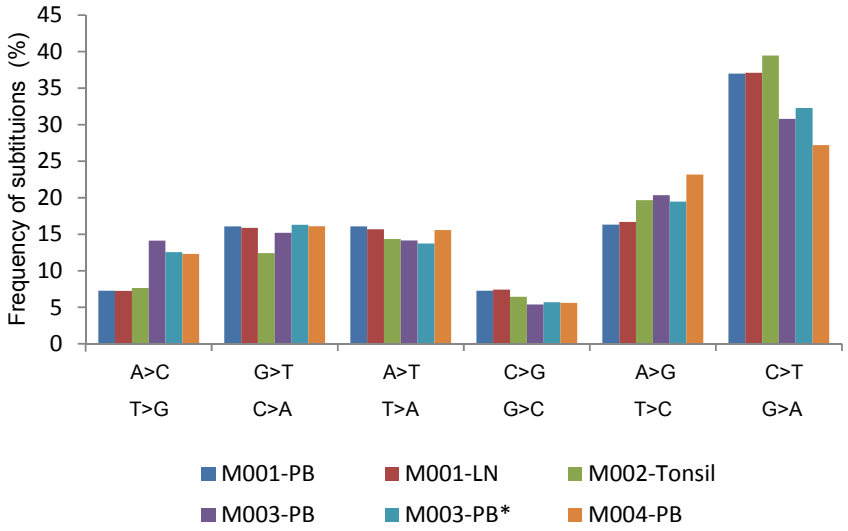

Fig. S2 *(A)* Profile of four MCL cases (six samples) analyzed by WGS and -WES. Distribution of somatic alterations (each case is represented in a different color), density of mutations per Mb in a 5 Mb window detected by WGS (vertical bars), protein-coding mutations (triangles) detected by WGS and WES, and copy number alterations (solid lines). The enlarged images show the acquired alterations of chromosomes 4 and 12 in the progressed M003 sample (gains in blue and losses in red). PB: peripheral blood, PB*: peripheral blood of progressed sample; LN: lymph node. *(B)* Rainfall plots showing regional clustering of somatic mutations (*kataegis*) in the four cases (six samples) analyzed by WGS. Mutations are represented on the X-axis from chromosome 1 to chromosome Y, and intermutation distance (in $\log_{10}$ bp) is drawn on the Y-axis. Clusters of mutations present lower intermutation distances (between 0 and 4).

A

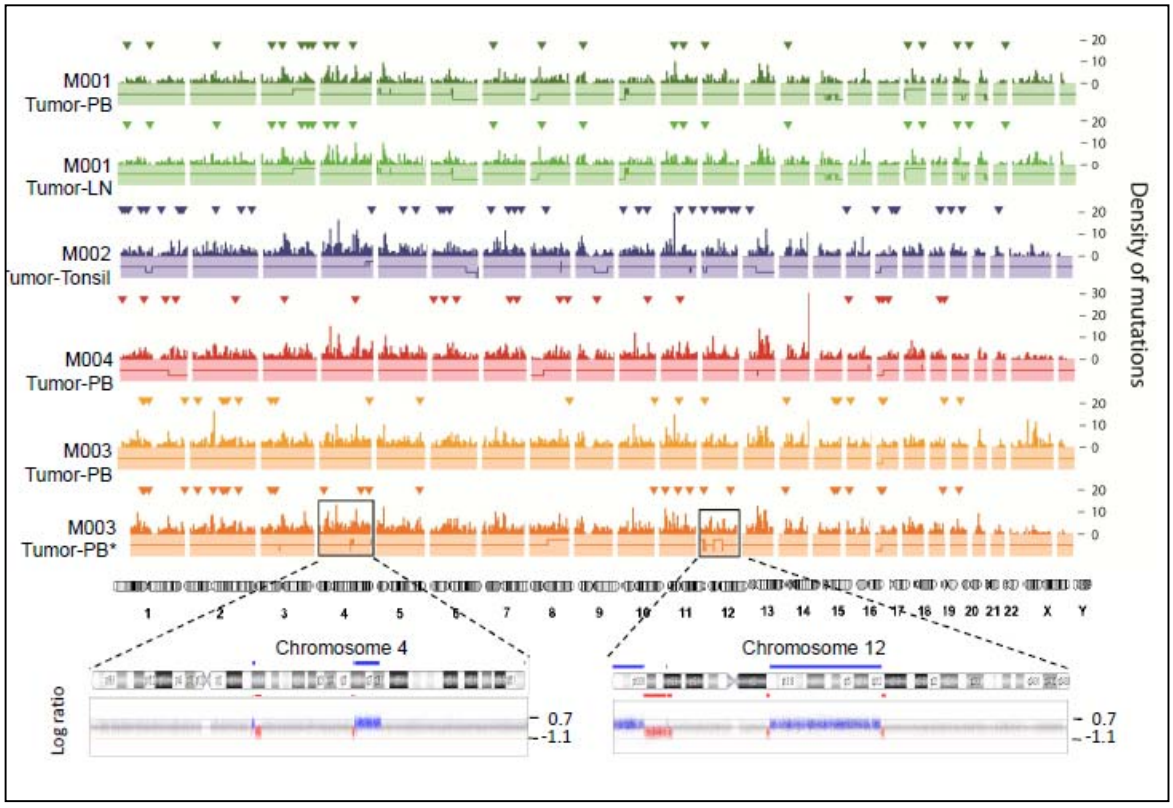

B

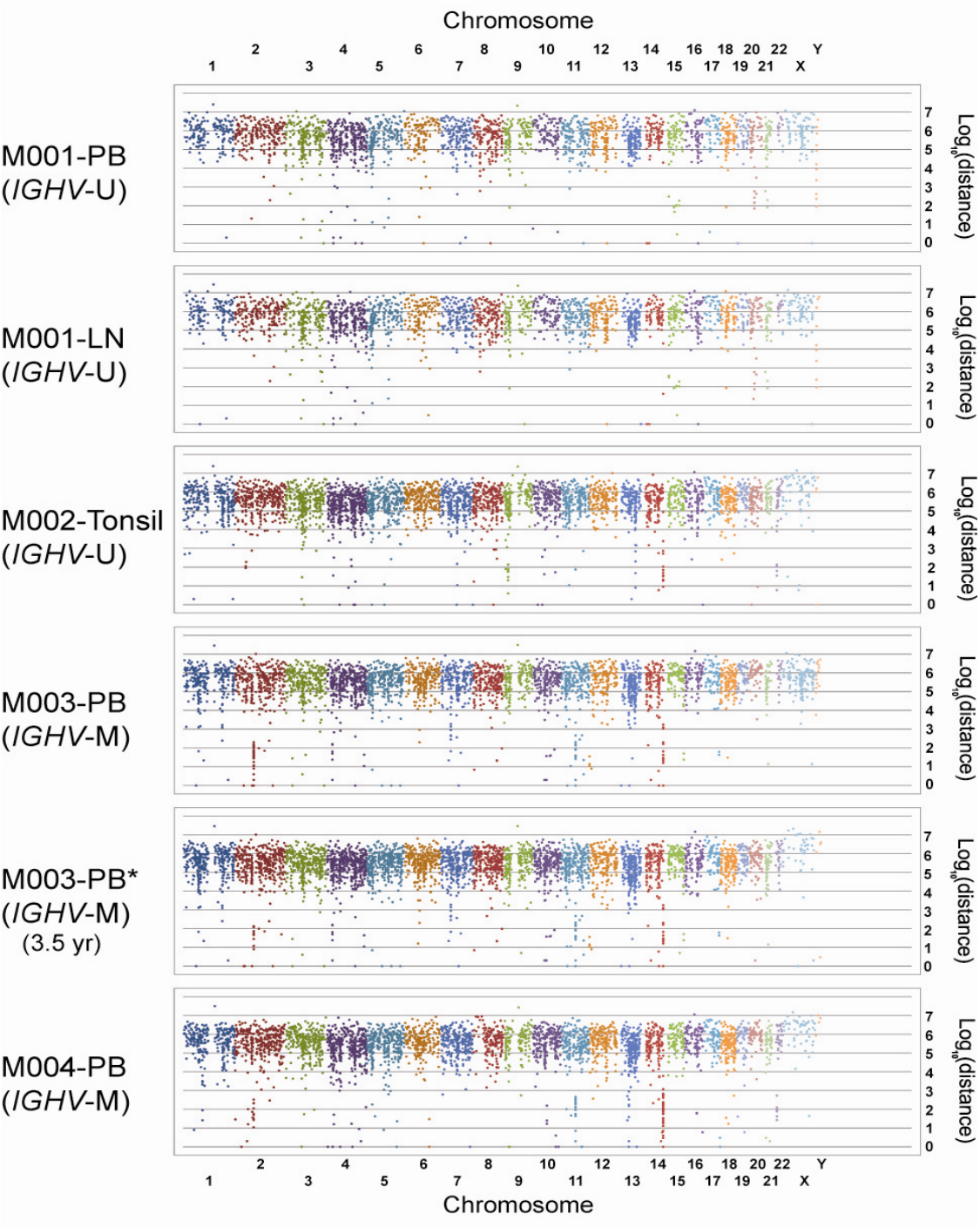
Chromosome
1 2 3 4 5 6 7 8 9 10 11 12 13 14 15 16 17 18 19 20 21 22 X Y
M001-PB (IGHV-U)
M001-LN (IGHV-U)
M002-Tonsil (IGHV-U)
M003-PB (IGHV-M)
M003-PB* (IGHV-M) (3.5 yr)
M004-PB (IGHV-M)
Log10(distance)
0 1 2 3 4 5 6 7
Chromosome

Fig. S3 *(A)* Chromosomal imbalances detected by high-resolution SNP-array in the 29 MCL cases from the WES series. On the X-axis the chromosomes are represented horizontally from 1 to 22, on the Y-axis the percentage of cases showing the CNAs. Gains are represented on the positive Y-axis and colored in blue, whereas losses are represented on the negative Y-axis in red. The most frequent CNA were gains of 3q21.3-q26.31 (9/29, 31%), 8q24.22-q24.3 (7/29, 24%), 12q13.13-q24.33 (4/29, 14%), 13q31 (7/29, 24%) and 18q21.33 (5/29, 17%) and losses of 1p21-p22 (13/29, 45%), 6q23.1-q24.2 (5/29, 17%), 9p21.3 (5/29, 17%, homozygous in 3 cases, zoomed in panel B), 9q21.31-q31.1 (5/29, 17%), 11q22-q23 (11/29, 38%), 13q (14/29, 48%) and 17p13.1 (6/29, 21%) (Table S10). Other homozyous deletions include 6q27, 13q14.2 and 13q32.1-q32.2 in single cases. In addition to copy number changes, 13 regions of acquired CNN-LOH were identified in 11 different patients (Table S10). Integration of CNA and somatic mutations revealed that only the recurrent losses/CNN-LOH of 17p and 11q were associated with mutations of *TP53* (five mutated cases with deletion and one with CNN-LOH), *ATM* (six mutated cases with deletion) and *BIRC3* (nine mutated cases with deletion). *CDNK2B* was the only gene targeted by recurrent homozygous deletions.

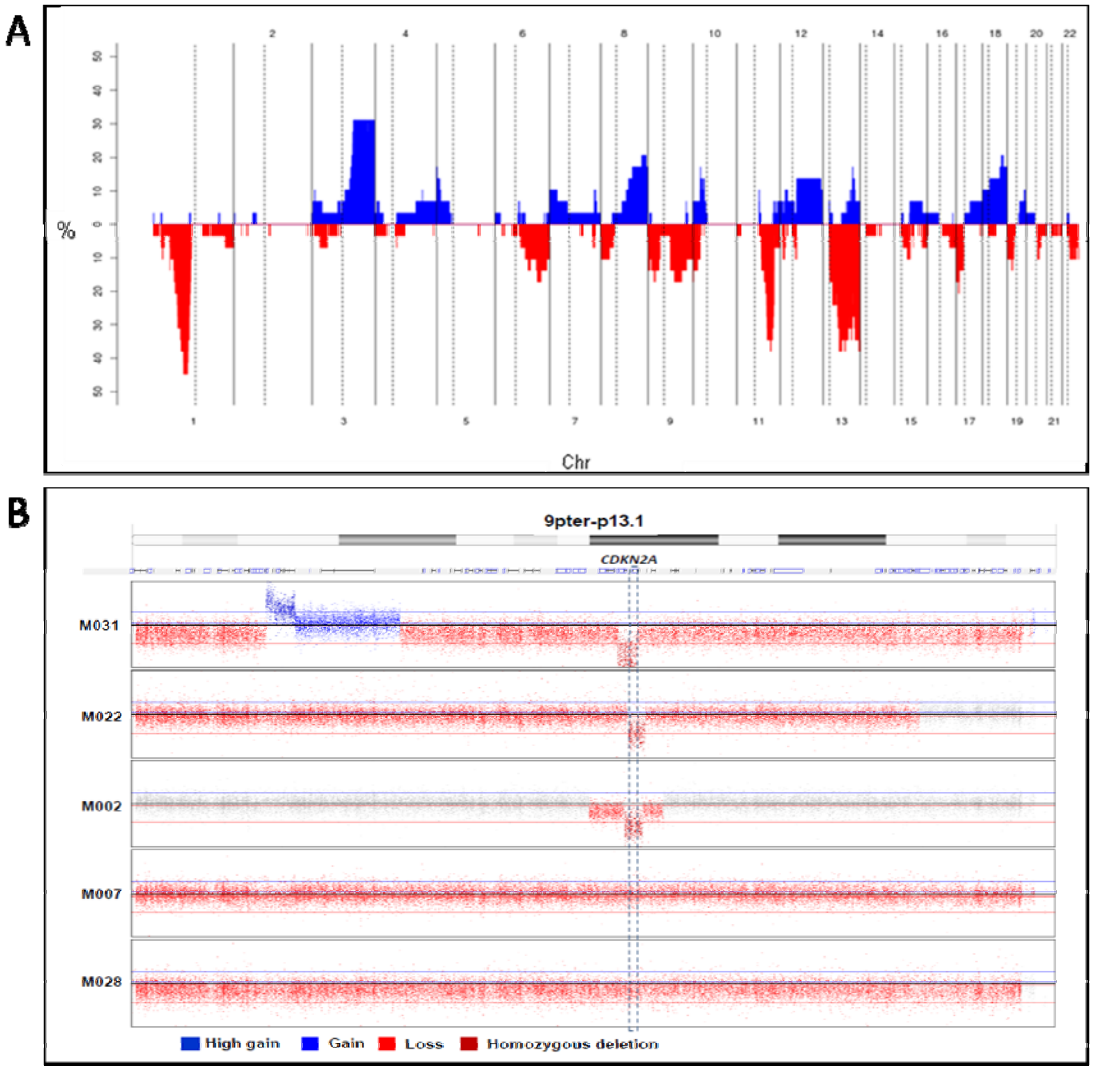

Fig. S4 *(A) BIRC3* and *ATM* mutations related to 11q copy number status by SNP-array in the 29 MCL analyzed by WES.

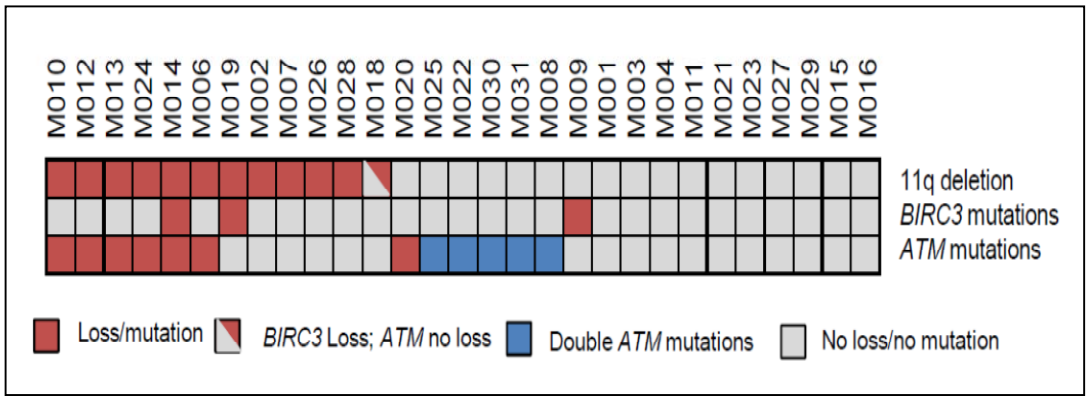

Fig. S5 *ATM* gene mutation distribution detected by WES in MCL of the present study (upper part) and MCL (10, 11) and CLL (4, 12-19) previously described (lower part).

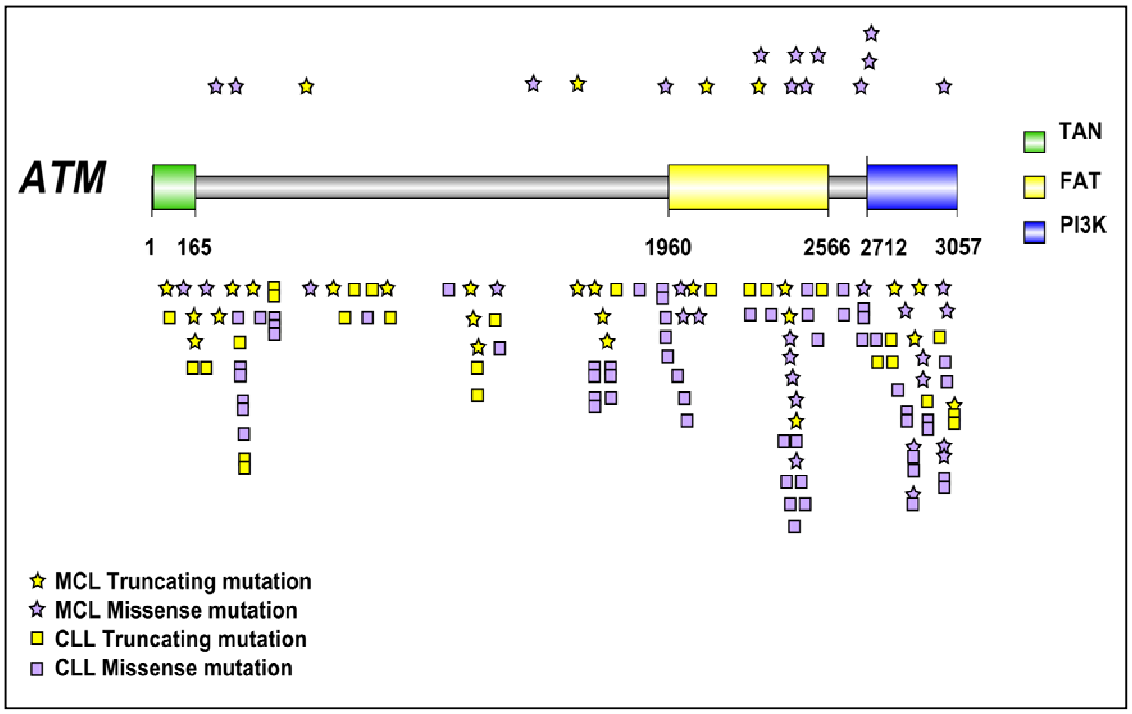

Fig. S6 *CCND1* gene mutation distribution detected by WES in MCL of the present study (upper part) and in MCL by RNA-sequencing previously described (20) (lower part).

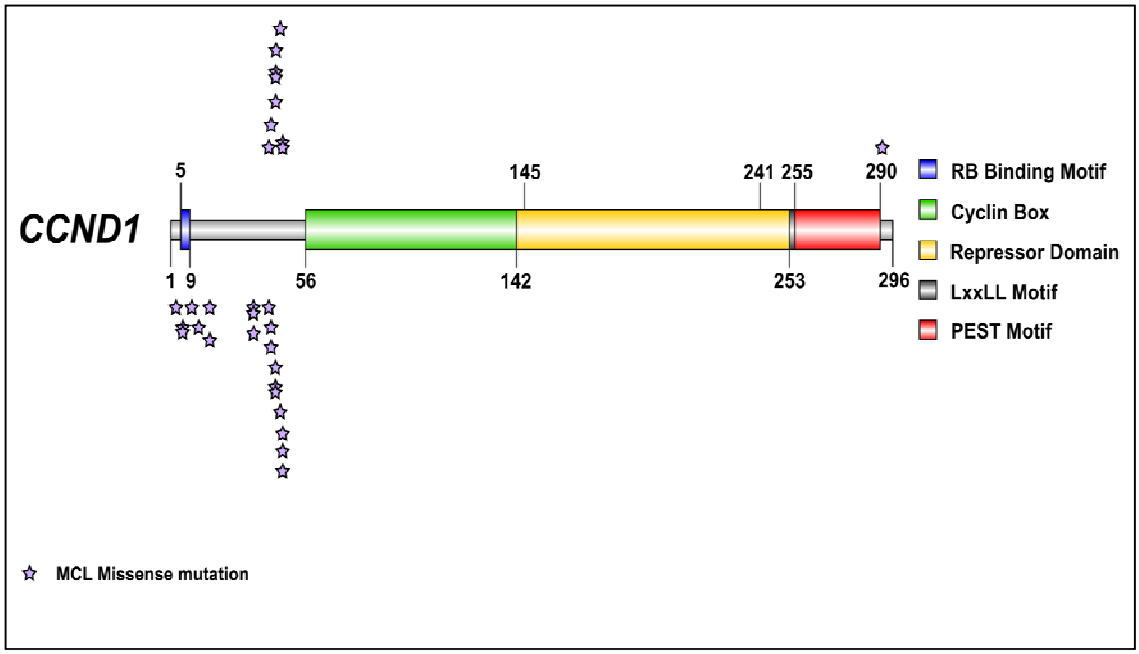

Fig. S7 Landscape of genetic variation in MCL. Heatmap of the recurrent mutations in MCL (cases in columns) detected by WES and Sanger sequencing in MCL. Only samples with 3 or more evaluable genes are presented. Molecular data include SOX11 expression (positive: green) and *IGHV* gene mutational status (unmutated: blue). The seven validated genes (mutated cases in orange) and recurrent CNA are shown, including 3q and 8q gains (red) and 9p, 11q losses and 17p loss and/or CNN-LOH (blue). Not available information is indicated in white.

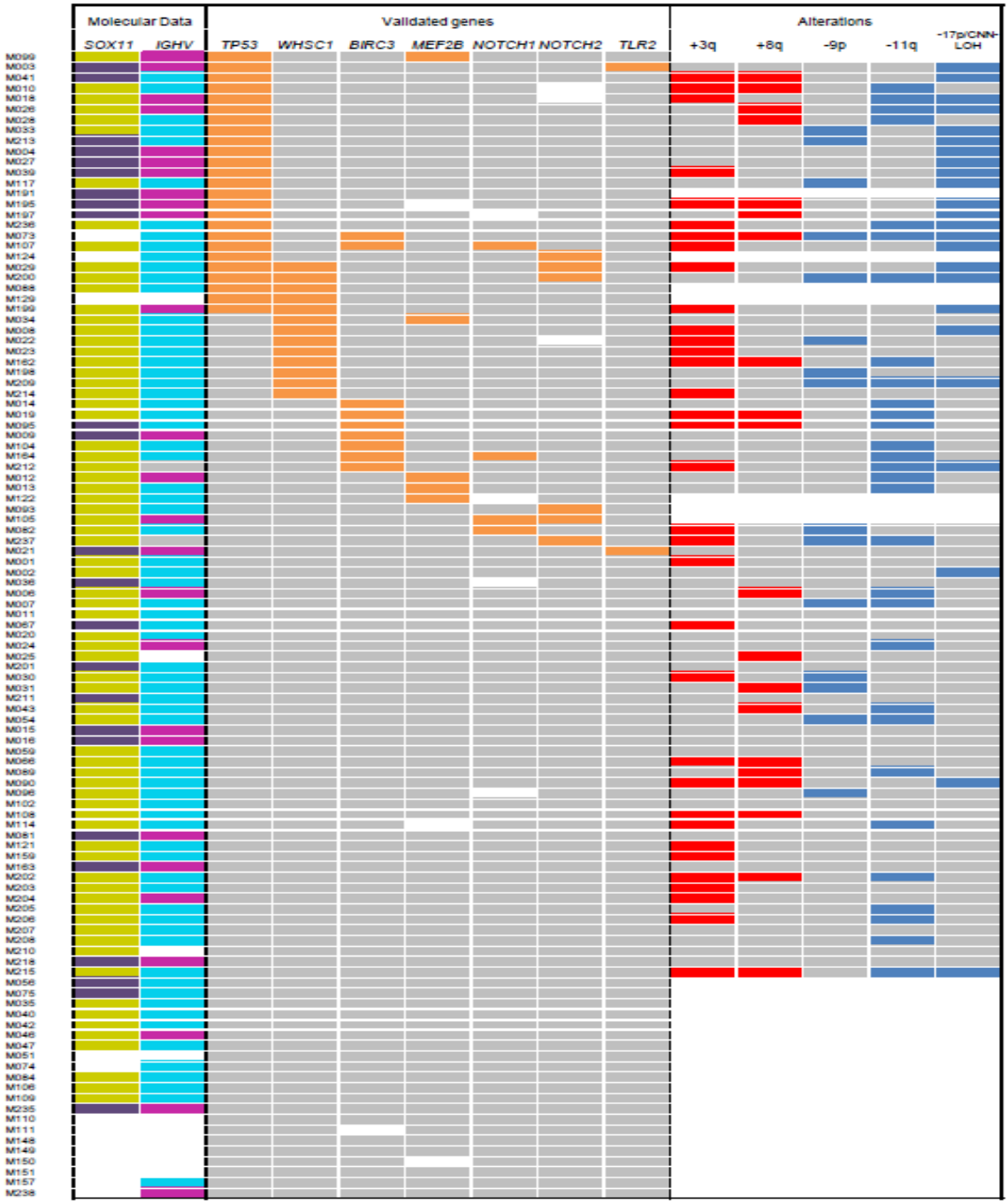

Fig. S8 Gene set enrichment analysis of 8 *WHSC1*-mutated and 31 -unmutated MCL cases using lymphoid gene expression signatures (21). *WHSC1*-mutated cases showed enrichment of gene signatures related to proliferation (Gene Set 1) (22), cell cycle (Gene Set 2) (23) and the t(4;14)-related signature (MS-cluster) (Gene Set 3) (24). In addition, *WHSC1*-mutated MCL showed significant overexpression of gene signatures associated with the *in vitro* overexpression of wild-type *WHSC1* in the KMS11 PCM cell line described in the supplementary Table S5 of the original paper (Gene Set 4) (25). The remaining two gene sets (Gene Set 5-6) were compiled from the reanalysis of the published gene expression profiling studies of the KMS11 PCM cell line transduced with the wild-type (Gene Set 5) or the gain-of-function exon 19-mutant *WHSC1* (Gene Set 6) (25). Interestingly, these two signatures were also significantly upregulated in the primary MCL with *WHSC1* mutations.

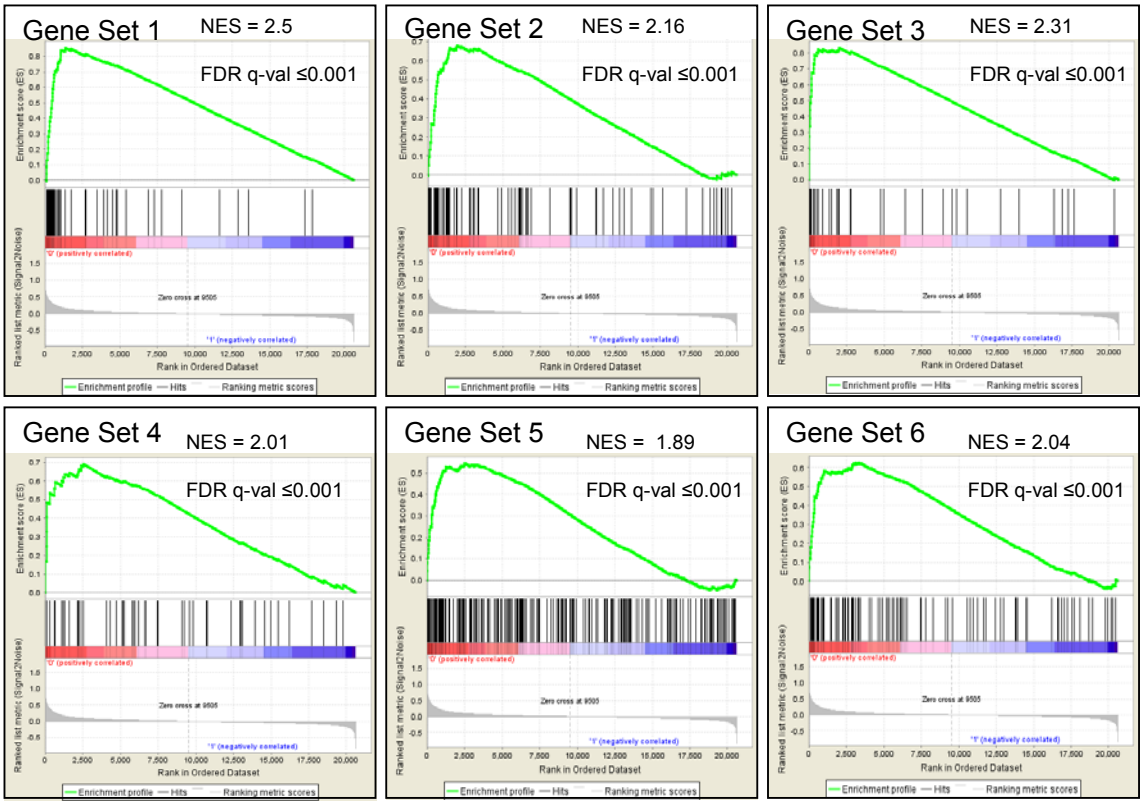

Fig. S9 *MLL2* gene mutation distribution detected by WES in MCL of the present study (upper part). In the lower part the previously described mutations in diffuse large B-cell lymphoma (DLBCL), follicular lymphoma (FL), and plasma cell myeloma (PCM) (26-29).

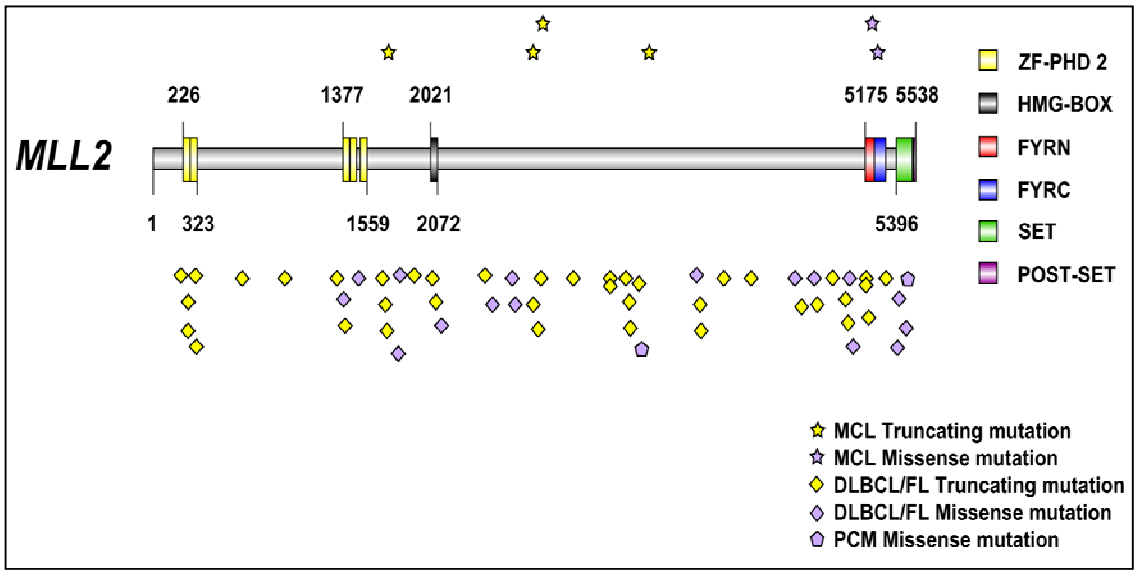

Fig. S10 *MEF2B* gene mutation distribution showing the location of the different somatic mutations identified by WES and Sanger sequencing in MCL in the present study (upper part) and in DLBCL/FL from the literature (lower part) (26, 27, 30, 31).

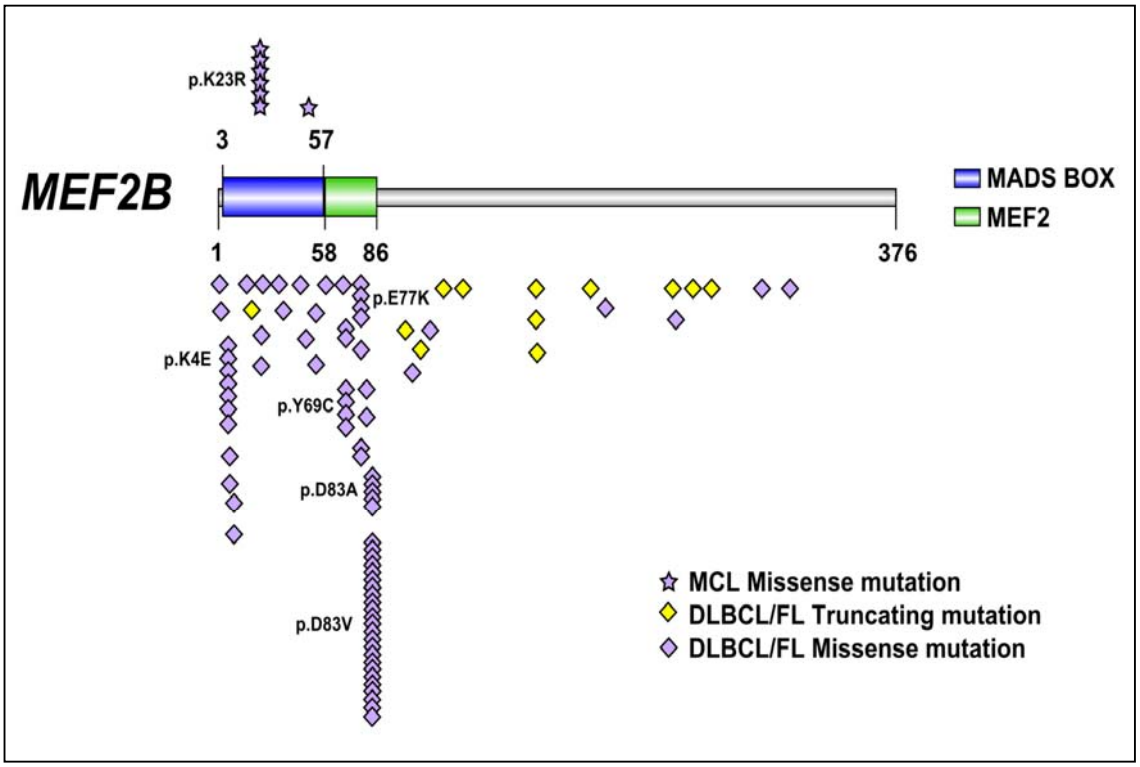

Fig. S11 Secretion of IL-8 (CXCL8) in *TLR2*-mutated and -unmutated tumors and healthy donors. Plot representing cytokine levels secreted by B cells before and after TLR2 stimulation with peptidoglycan (PGN) from *S. aureus* (PGN-SA). 'p.D327V' corresponds to tumor cells from one MCL and one CLL carrying this mutation. 'p.Y298S' corresponds to a MCL patient with this *TLR2* mutation. The values for 3 CLL cases, 4 MCL, and 4 normal B cells are represented as the mean value. Standard error is indicated in bars.

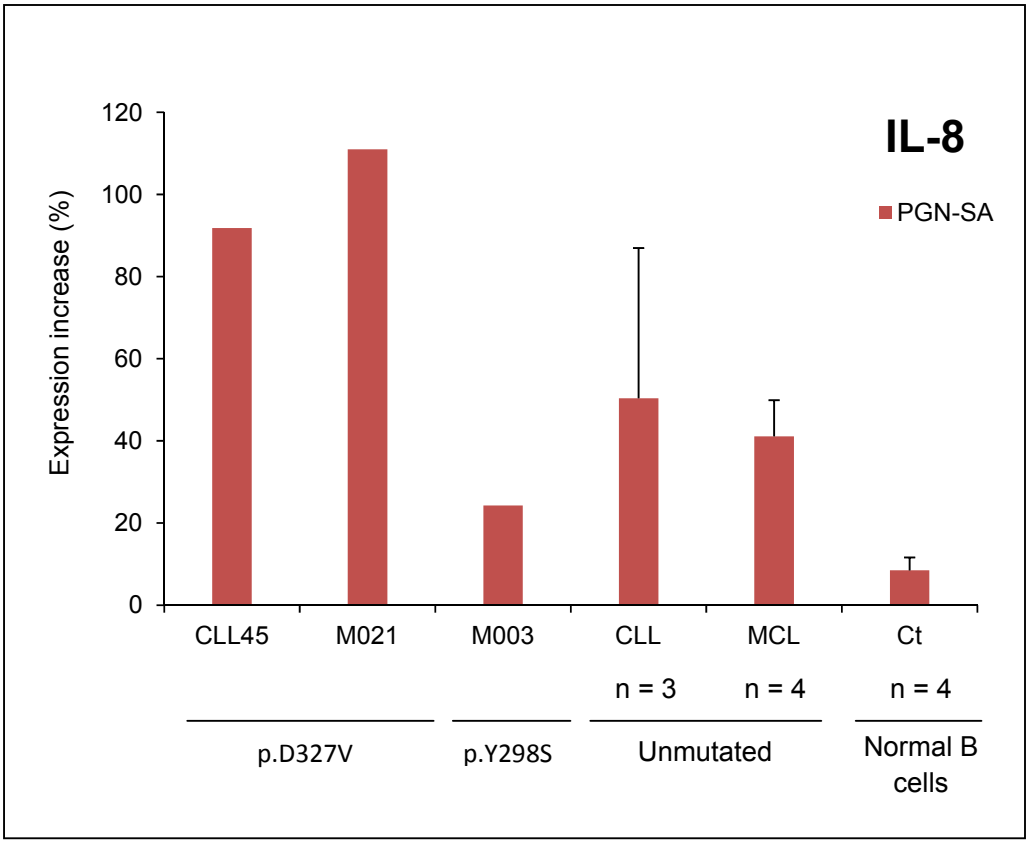

Fig. S12 Gene set enrichment analysis of 2 *NOTCH2*-mutated and 19 -unmutated cases. The plots show that *NOTCH2*-mutated samples displayed a significant overexpression of three sets of genes upregulated by NOTCH activation in lymphoid cells: Gene Set 1 (32), Gene Set 2 (33), Gene Set 3 (34). *NOTCH2*-mutated tumors also show underexpression of a gene signature upregulated following NOTCH inhibition (Gene Set 4) (35). Similarly, two gene sets up (Gene set 5) and downregulated (Gene Set 6) by NOTCH-inhibition in MCL cell lines (20) were inversely modulated in the *NOTCH2*-mutated MCL.

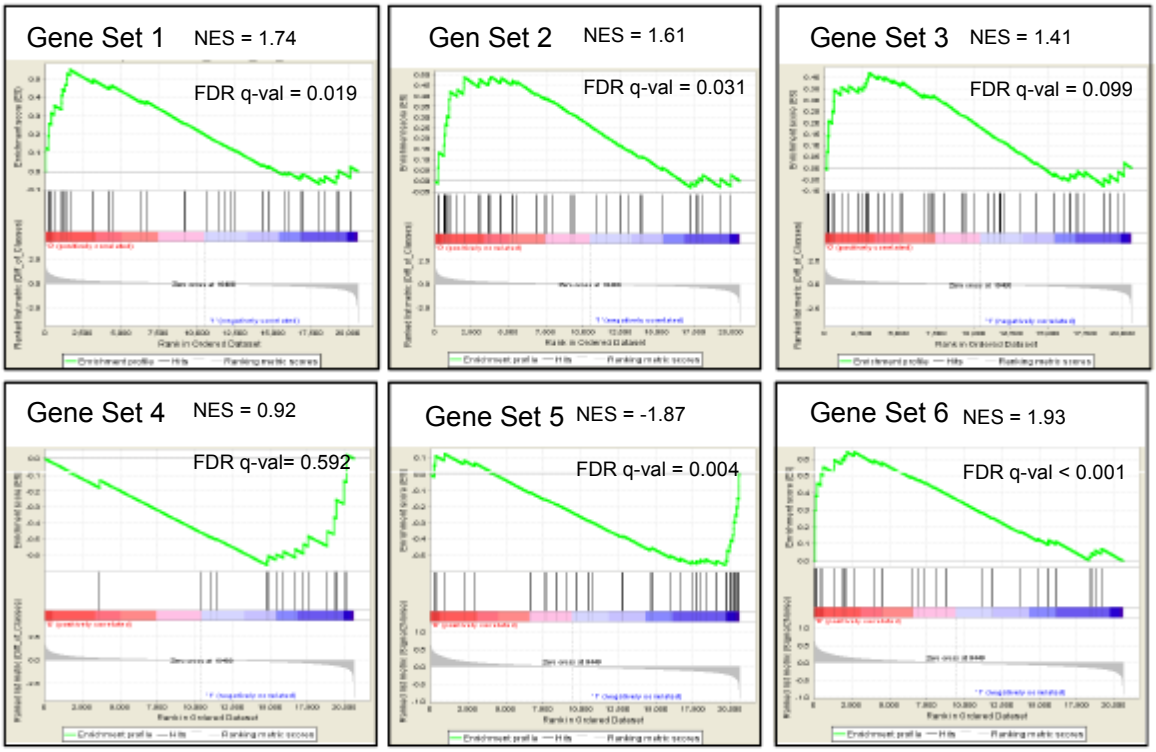

Fig. S13 Actuarial probability of overall survival of MCL patients according to the combination of both *NOTCH2* and *TP53* mutations. Of note, regardless of *TP53* mutational status patients with *NOTCH2* mutations had a dismal prognosis.

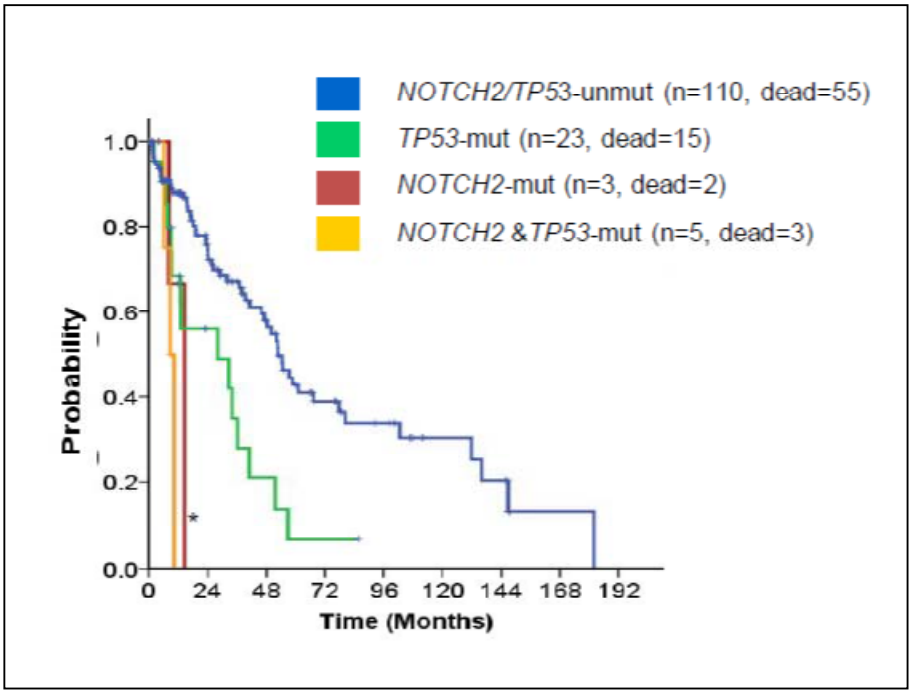

Fig. S14 *NOTCH1* gene mutation distribution showing the location of the different somatic mutations identified by Sanger sequencing in MCL of the present study (upper part) and in MCL (20), splenic marginal zone lymphoma (36), CLL/Richter Syndrome (3, 37, 38) and DLBCL/FL from the literature (lower part) (26-28).

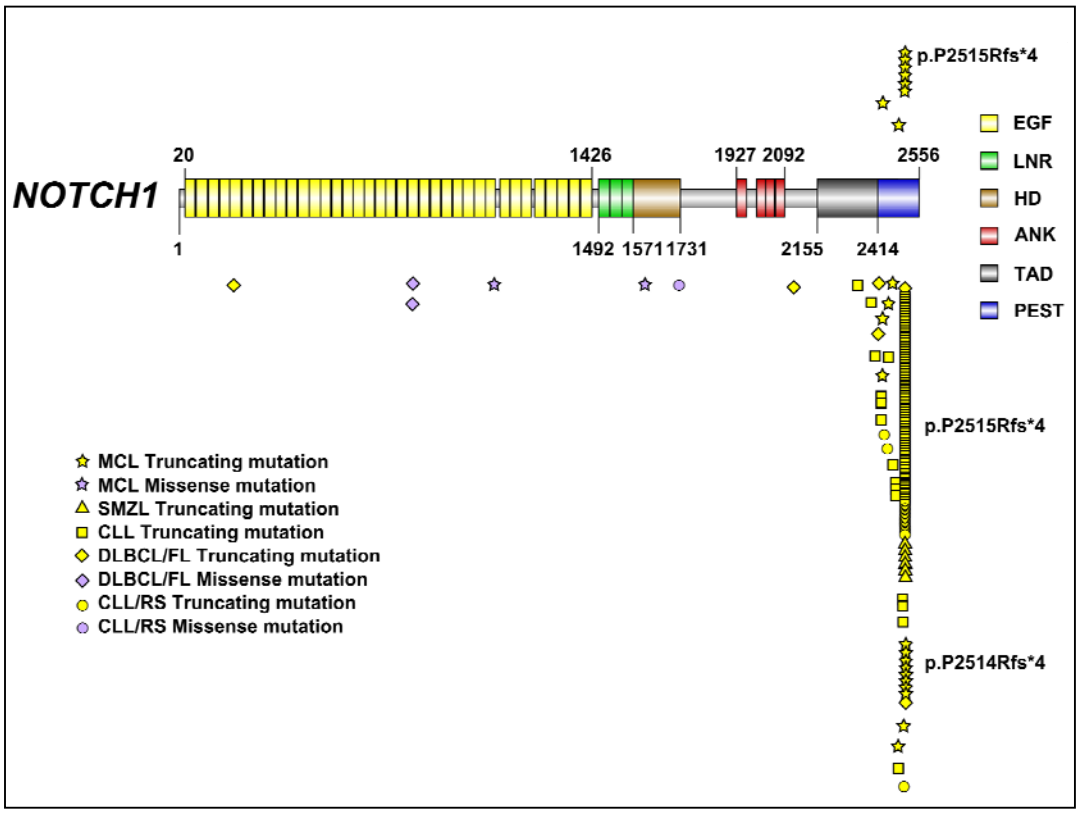

Fig. S15 Actuarial probability of overall survival of MCL patients with mutated or unmutated *NOTCH1* (*P*=0.026).

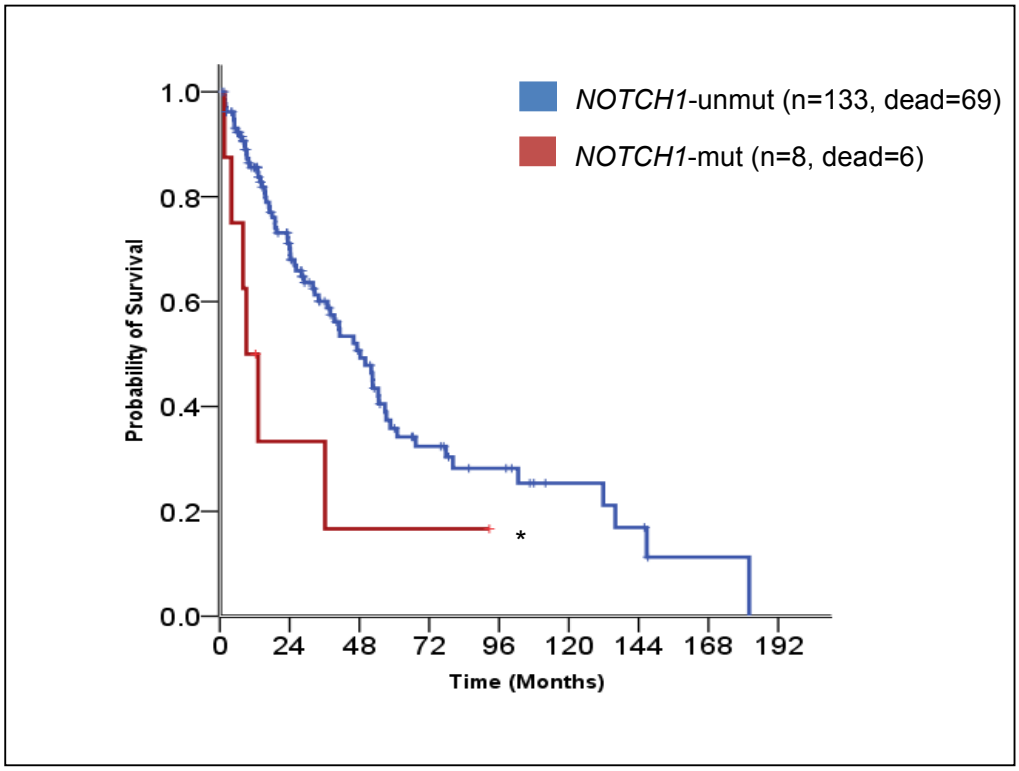

Fig. S16 Mutational analysis in progressed and synchronic samples of the validation series. The mutated genes are highlighted in red whereas the unmutated genes are grey-colored, white indicates not available. *(A)* Analysis of mutations of 7 genes in 11 MCL cases with samples at two time points. Sample with asterisk (*) indicates the progressed/post-treatment sample, the interval of time between samples is indicated in months. *(B)* Analysis of mutations of 7 genes in 8 MCL cases with synchronic tumor samples affecting different topographic sites. (LN, lymph node; peripheral blood). *BIRC3* mutation was acquired in the relapsed sample of two patients (M009 and M164). Only sample M009-PB* was used for WES analysis, all the remaining samples correspond to the validation series.

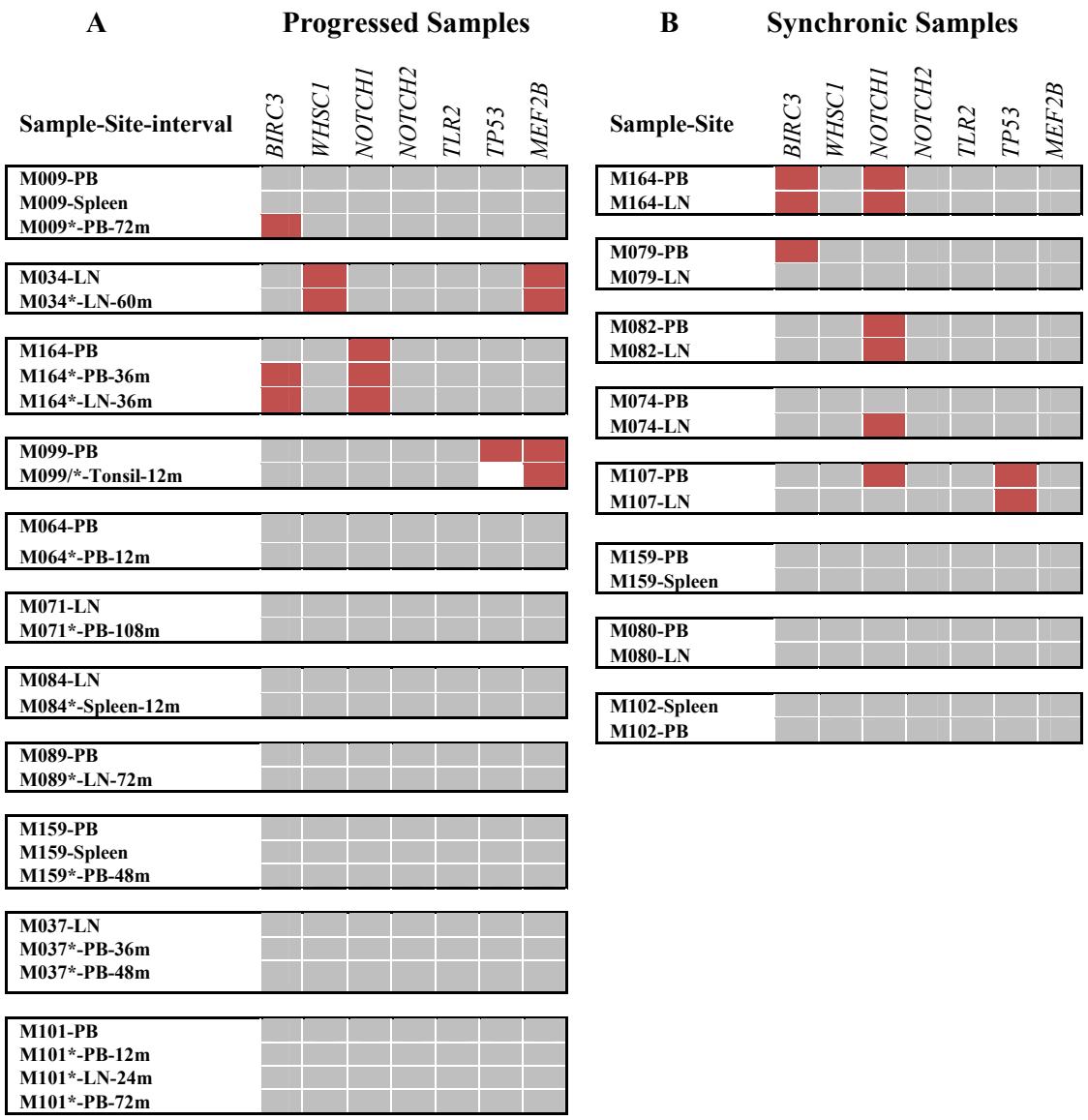

SUPPLEMENTARY TABLES

Table S1. Details of the 29 MCL patients analyzed by WGS and/or WES.

Case	Sample	Sampling Time	Synchronic/ At progression	Cytology	Purity	WGS	WES	SNP-array	GEP	SOX11	*IGHV* gene	% *IGHV*
M001	PB normal				96	y	y	y				
M001	LN tumor	At diagnosis	Synchronic	Classic	>90	y	y	y		Pos	*IGHV3-21*	98.8
M001	PB tumor	At diagnosis	Synchronic		96.1	y	y	y	y	Pos		
M002	PB normal				99	y	y	y				
M002	Tonsil tumor	At diagnosis		Blastoid	>90	y	y	y	y	Pos	*IGHV4-34*	99.55
M002	PB tumor	Post-treatment	Relapse (3.2 yr)		96		y	y		Pos		
M003	PB normal				100	y	y	y				
M003	PB tumor	At diagnosis		Small cell	96	y	y	y	y	Neg	*IGHV3-23*	93.72
M003	PB tumor	Pre-treatment	Progression (3.5 yr)	Pleomorphic	98	y	y	y		Neg		
M004	PB normal				99.5	y	y	y				
M004	PB tumor	At diagnosis		Classic	99.7	y	y	y		Neg	*IGHV1-8*	96.99
M006	PB normal				99.5	y	y	y				
M006	PB tumor	At diagnosis		Classic	95	y	y	y	y	Pos	*IGHV4-31*	96.9
M007	PB normal				99.7		y	y				
M007	Colon tumor	At diagnosis		Classic	>90		y	y		Pos	*IGHV4-34*	99.65
M008	PB normal				99		y	y				
M008	PB tumor	Pre-treatment		Classic	90		y	y	y	Pos	*IGHV1-8*	99.31
M009	PB normal				99.9		y	y				
M009	PB tumor	At diagnosis			99			y		Neg	*IGHV3-9*	92.36
M009	PB tumor	Post-treatment	Progression (5 yr)	Small cell	98		y	y	y	Neg		
M010	PB normal				98		y	y				
M010	LN tumor	At diagnosis	Synchronic	Classic	>90		y	y		Pos	*IGHV1-8*	100
M010	PB tumor	At diagnosis	Synchronic		100		y	y	y	Pos		
M011	PB normal				99		y	y				
M011	LN tumor	At diagnosis		Classic	>90		y	y		Pos	*IGHV1-8*	98.83
M012	PB normal				100		y	y				
M012	LN tumor	At diagnosis		Classic	82		y	y	y	Pos	*IGHV3-7*	96.18
M013	PB normal				99.8		y	y				
M013	LN tumor	At diagnosis		Classic	75		y	y	y	Pos	*IGHV3-23*	99.31
M014	PB normal				100		y	y				
M014	LN tumor	At diagnosis		Classic	89		y	y	y	Pos	*IGHV4-59*	100

M015	PB normal				99.33	y	y				
M015	PB tumor	Untreated		Small cell	85.2	y	y	y	Neg	*IGHV1-2*	96.53
M016	PB normal				95.5	y	y				
M016	Spleen Tumor	Untreated	Synchronic	Small cell	89	y	y		Neg	*IGHV4-39*	92.04
M016	PB tumor	Pre-treatment	Synchronic		97.2	y	y	y	Neg		
M018	PB normal				99.5	y	y				
M018	PB tumor	Post-treatment		Classic	99.5	y	y		Pos	*IGHV3-23*	93.75
M019	PB normal				97.5	y	y				
M019	PB tumor	At diagnosis		Blastoid	99	y	y		Pos	*IGHV1-18*	99.25
M020	PB normal				99	y	y				
M020	PB tumor	At diagnosis		Classic	84	y	y		Pos	*IGHV3-21*	97.41
M021	PB normal				99.5	y	y				
M021	PB tumor	Untreated		Small cell	99	y	y	y	Neg	*IGHV1-8*	94.44
M022	PB normal				100	y	y				
M022	LN tumor	Post-treatment		Blastoid	>90	y	y	y	Pos	*IGHV1-8*	100
M023	PB normal				97.6	y	y				
M023	LN tumor	At diagnosis	Synchronic	Classic	>90	y	y	y	Pos	*IGHV3-21*	99.59
M023	PB tumor	At diagnosis	Synchronic		96.9	y	y		Pos		
M024	PB normal				98	y	y				
M024	LN tumor	At diagnosis		Blastoid	80	y	y	y	Pos	*IGHV4-4*	95.24
M025	PB normal				99	y	y				
M025	LN tumor	Untreated		Classic	65	y	y	y	Pos	n.a.	n.a.
M026	PB normal				99.9	y	y				
M026	LN tumor	At diagnosis	Synchronic	Classic	50	y	y		Pos	*IGHV4-59*	95.09
M026	PB tumor	At diagnosis	Synchronic		99.5	y	y	y	Pos		
M027	PB normal				98.4	y	y				
M027	PB tumor	Untreated		Small cell	98.9	y	y	y	Neg	*IGHV1-8*	96.88
M028	PB normal				99.5	y	y				
M028	PB tumor	At diagnosis		Classic	87	y	y	y	Pos	*IGHV3-23*	100
M029	PB normal				99.3	y	y				
M029	PB tumor	At diagnosis		Blastoid	99.3	y	y	y	Pos	*IGHV4-59*	98.25
M030	PB normal				99.4	y	y				
M030	PB tumor	At diagnosis		Classic	99.7	y	y	y	Pos	*IGHV3-11*	98.26
M031	PB normal				100	y	y				
M031	LN tumor	At diagnosis	Synchronic	Blastoid	98	y	y		Pos	*IGHV3-9*	100
M031	PB tumor	At diagnosis	Synchronic		95	y	y		Pos		

Abbreviations: IGHV, immunoglobulin heavy chain gene; GEP, gene expression profile; LN, lymph node; Neg.: negative; n.a., not available; PB, peripheral blood; Pos., positive; WGS, whole genome sequencing; Y, yes; yr, years.

Table S2. Clinicobiological features of the 4 patients (6 samples) analyzed by WGS.

	M001*	M002	M003	M003†	M004
DEMOGRAPHICS					
Age (years)	63	79	75	79	81
Gender	Male	Male	Male	Male	Male
MOLECULAR AND PATHOLOGICAL DATA					
Cytological variant	Classic	Blastoid	Small cell	Pleomorphic	Classic
CD5	Positive	Positive	Negative	Negative	Positive
CD23	Negative	Negative	Negative	Negative	Low positive
Ki-67 (%)	50	85	NA	NA	NA
SOX11	Positive	Positive	Negative	Negative	Negative
***IGHV* gene**	*IGHV3-21*	*IGHV4-34*	*IGHV3-23*	*IGHV3-23*	*IGHV1-8*
% *IGHV* identity	98.8	99.55	93.72	93.72	96.99
Number of CNA	23	11	1	22	6
Sample analyzed	LN/PB*	Tonsil	PB	PB	PB
DNA at diagnosis	Yes	Yes	Yes	No (3.5 years)	Yes
CLINICAL FEATURES AND OUTCOME					
ECOG (≥2)	Yes	No	No	Yes	No
B-symptoms	No	Yes	No	No	No
Ann Arbor Stage	IV	I	IV	IV	IV
Lymph nodes (>1cm)	Yes	No	No	No	No
Palpable splenomegaly	Yes	No	No	No	No
Bone marrow involvement	Yes	No	Yes	Yes	Yes
Lymphocytes ($x10^9$)	36	1.5	9	18.5	40
Leukocytes ($x10^9$)	38.7	8.3	13.3	18.9	46.8
LDH (>ULN)	Yes	No	No	No	No
β2-Microglobulin (>ULN)	Yes	No	No	Yes	Yes
MIPI Risk	High	High	Low	High	High
Treatment	R-CHOP	CHOP	Untreated	R-COP	CLB
Response	Failure	CR	-	CR	Failure
Status (OS, months) ‡	Dead (9)	Dead (39)	Alive (86+)	Alive (47+)	AWD (23+)

Abbreviations: AWD: alive with disease; CHOP , Cyclophosphamide, doxorubicin, vincristine and prednisone; CLB, Chlorambucil; CR, complete response; ECOG, Eastern Cooperative Oncology Group; IPI, International Prognostic Index; LDH, Lactate dehydrogenase; MIPI, Mantle cell lymphoma International Prognostic Index; NA, not applicable; ULN, upper level of normal; WGS, whole genome sequencing.

*Two synchronic tumor samples from peripheral blood (PB) and lymph node (LN) were sequenced.

†Sample M003 corresponds to the sequential sample of patient M003 obtained 3.5 years after diagnosis at the moment of progression of the patient.

‡OS from sampling.

Table S3. Clinicobiological features of the 29 MCL patients analyzed by WES and the 172 patients included in the validation series.

Variable	Category	WES Series (n=29)	Validation Series (n=172)
DEMOGRAPHICS			
Age at diagnosis	Median (range)	67 (48-89)	66 (35-89)
Gender	Male	21	133
MOLECULAR AND PATHOLOGICAL DATA			
Cytological variant	Blastoid/pleomorphic	7/29 (24%)	23/133 (17%)
CD5	Positive	21/28 (72%)	92/98 (94%)
CD23	Negative	21/28 (75%)	51/66 (77%)
Ki-67	High (≥30%)	9/20 (45%)	28/89 (31%)
SOX11	Positive	22/29 (76%)	85/116 (73%)
IGHV	Unmutated (>97%)	16/28 (57%)	90/124 (73%)
CNA	Mean (SD)	9.93 (9.36)	9.32 (9.56)
CLINICAL FEATURES AND OUTCOME			
ECOG	≥2	7/23 (30%)	25/80 (31%)
B-symptoms		4/23 (17%)	29/83 (35%)
Ann Arbor Stage	IV	23/29 (79%)	89/97 (92%)
Lymph nodes	(>1 cm)	17/28 (61%)	107/143 (75%)
Palpable splenomegaly		10/28 (36%)	76/125 (61%)
Bone marrow involvement		21/23 (91%)	84/90 (93%)
LDH	(>ULN)	8/27 (30%)	39/93 (41%)
β2-Microglobulin	(>ULN)	19/26 (73%)	53/76 (70%)
MIPI Risk	High	15/24 (63%)	46/69 (67%)
Treatment	No treatment	5/29 (17%)	14/139 (11%)
	Conventional*	14/29 (42%)	101/139 (73%)
	High dose AraC or HDT	9/29 (31%)	10/139 (7%)
	Rituximab at any time	19/26 (73%)	49/121 (40%)
Response	Complete response	16/24 (67%)	21/80 (26%)
	Partial response	5/24 (21%)	32/80 (40%)
Follow-up (months)	Median (range)	12.8 (6-147)	43.25 (0.4-195)
Overall survival (months)	Median (95% CI)	77 (15-100)	52 (45-58)
Status	Dead	10/29 (34%)	100/165 (61%)
Time of sampling	At diagnosis	20/29 (69%)	126/159 (79%)
	Pre-treatment	6/29 (21%)	11/159 (7%)
	Progression/Relapse	3/29 (10%)	22/159 (14%)
Sample analyzed (site)†	PB	22/37 (60%)	80/194 (41%)
	LN	12/37 (32%)	81/194 (42%)
	Spleen	1/37(3%)	12/194 (6%)
	Others	2/37 (5%)	21/194 (11%)

Abbreviations: CNA, copy number alterations; CI, confidence interval; F, female; LDH, Lactate dehydrogenase; MIPI, Mantle cell lymphoma International Prognostic Index; SD, standard deviation; ULN, upper level of normal.

*Conventional treatment included CHOP or CHOP-like regimens in the majority of cases (67%) and in a lesser extent alkylators-only or fludarabine based combinations.

†Samples of patients analyzed at different time points or different topographic sites are considered.

Table S4. Characteristics and authentication of the six MCL cell lines analyzed by WES.

	JVM-2	JEKO-1	MAVER-1	MINO	REC-1	Z138
Gender	Female	Female	Male	Female	Male	Male
CD5	Positive	Positive	Positive	Positive	Negative	Negative
CD23	Positive	Negative	Negative	Negative	Negative	Negative
SOX11	Negative	Positive	Positive	Positive	Positive	Positive
EBV	Positive	Negative	Negative	Negative	Negative	Negative
CNA	8	79	47	22	37	25
Ploidy	2n	3n+	2n	3n+	2n-	2n
MYC	Wt	Amp	Wt	Wt	Wt	Wt
BCL2	Wt	Gain	Amp	Amp	Wt	Amp
CCND1	Transl.	Transl.	Transl./Amp	Transl.	Transl.	Transl.
***IGHV* gene**	*IGHV3-9*	*IGHV2-70*	*IGHV3-9*	*IGHV3-21*	*IGHV1-2*	*IGHV1-8*
% *IGHV* identity	100	99.66	100	98.6	98.61	98.96
D5S818*	11-12	10-13	12-12	11-12	12-13	11-13
D13S317*	11-13	8-9	8-13	12-12	10-10	9-12
D7S820*	10-11	10-11	8-8	10-11	10-11	8-8
D16S539*	12-13	12-12	9-12	11-12	11-11	11-11
VWA*	17-17	14-14	14-18	14-17	17-17	15-18
TH01*	6-9	7-7	8-9	9.3- 9.3	9- 9.3	6-6
AM*	X-X	X-X	X-Y	X-Y	X-Y	X-Y
TPOX*	8-11	8-8	8-12	8-11	8-9	8-8
CSF1PO*	11-11	9-12	10-11	9-11	10-12	10-11

Abbreviations: Amp., Amplification; CNA, copy number alterations; EBV, Epstein-Barr virus; Transl., translocation; Wt: wild type (no gain, no loss, no translocation).

*The cell line identity was authenticated by analyzing 9 alleles with PowerPlex 1.2 kit (Promega) and using an on-line STR profile maintained by **Deutsche Sammlung von Mikroorganismen und Zellkulturen (**DSMZ) (http://www.dsmz.de/services/services-human-and-animal-cell-lines/online-str-analysis.html). All cell lines were negative for mycoplasma contamination test. JVM-2, JEKO- 1 and MINO were purchased at ATCC. MAVER-1, REC-1 and Z138 were kindly provided by Dr. A. Zamo (Verona, Italy), Dr. Bastard (Rouen, France) and Dr. E. Ortega-Paino (Sweden), respectively.

Table S5. Statistics of the four MCL analyzed by WGS.

Case	Sample	Number of reads mapped	Depth	Callability (≥10 reads)
M001	Normal	927,200,649	25X	95.24
	Tumor-PB	804,035,210	29X	94.53
	Tumor-LN	1,512,779,314	50X	99.43
M002	Normal	1,236,000,961	39X	99.28
	Tumor-Tonsil	1,682,828,406	52X	99.3
M003	Normal	1,780,104,841	56X	99.7
	Tumor-PB	1,971,489,271	69X	99.65
	Tumor-PB*	2,295,624,016	59X	99.63
M004	Normal	1,631,707,336	54X	99.64
	Tumor-PB	1,747,697,204	54X	99.6

Abbreviations: LN, Lymph node; PB, peripheral blood.
*Pre-treatment progressed sample of patient M003 after 3.5 years.

Table S6. Statistics of the 37 tumor samples, their 29 corresponding normal DNA, and six MCL cell lines analyzed by WES.

Case	Sample	Number of reads mapped	Depth	Callability (≥10 reads)
M001	Normal	95,779,162	80X	87.14%
	Tumor-PB	120,654,496	103X	88.12%
	Tumor-LN	95,779,162	93X	88.73%
M002	Normal	123,225,998	109X	90.11%
	Tumor-Tonsil	90,828,297	81X	89.09%
	Tumor-PB*	82,115,112	73X	85.28%
M003	Normal	76,169,653	67X	86.55%
	Tumor-PB	108,481,777	97X	89.14%
	Tumor-PB*	97,100,344	87X	88.51%
M004	Normal	84,767,438	76X	87.34%
	Tumor-PB	85,970,578	81X	87.40%
M006	Normal	81,218,737	67X	86.49%
	Tumor-PB	75,579,744	62X	83.21%
M007	Normal	88,771,344	76X	88.43%
	Tumor-Colon	97,448,384	77X	87.74%
M008	Normal	111,347,503	98X	88.74%
	Tumor-PB	115,253,745	105X	88.61%
M009	Normal	123,080,801	99X	87.90%
	Tumor-PB	111,038,294	89X	87.59%
M010	Normal	99,020,306	75X	85.38%
	Tumor-PB	82,125,287	69X	85.29%
	Tumor-LN	133,192,890	102X	88.65%
M011	Normal	90,848,586	73X	86.11%
	Tumor-LN	97,638,239	75X	86.06%
M012	Normal	106,309,955	85X	87.06%
	Tumor-LN	120,019,051	96X	87.49%
M013	Normal	103,462,261	85X	87.48%
	Tumor-LN	111,265,949	90X	86.76%
M014	Normal	93,672,497	76X	86.30%
	Tumor-LN	128,802,461	103X	88.32%
M015	Normal	117,177,410	94X	87.93%
	Tumor-PB	117,299,513	96X	88.07%
M016	Normal	77,156,805	63X	84.30%
	Tumor-PB	81,110,925	62X	84.30%
	Tumor-Spleen	74,399,590	64X	86.96%
M018	Normal	91,677,570	73X	84.94%
	Tumor-PB	96,710,099	76X	85.67%
M019	Normal	89,761,722	76X	87.08%
	Tumor-PB	104,490,136	87X	87.60%
M020	Normal	109,514,955	93X	88.46%
	Tumor-PB	99,839,051	83X	88.52%

M021	Normal	70,547,300	56X	84.13%
	Tumor-PB	82,048,947	65X	85.91%
M022	Normal	72,584,193	62X	85.69%
	Tumor-LN	77,277,173	61X	85.67%
M023	Normal	97,654,402	87X	88.46%
	Tumor-PB	87,685,153	77X	87.48%
	Tumor-LN	112,118,398	97X	89.46%
M024	Normal	68,869,934	60X	87.15%
	Tumor-LN	45,120,771	40X	82.85%
M025	Normal	99,991,928	90X	88.78%
	Tumor-LN	74,270,156	64X	86.77%
M026	Normal	83,435,018	72X	88.17%
	Tumor-PB	89,355,122	80X	88.17%
	Tumor-LN	87,973,822	75X	87.95%
M027	Normal	107,534,375	91X	88.82%
	Tumor-PB	83,413,356	71X	88.22%
M028	Normal	95,178,168	82X	88.42%
	Tumor-PB	83,686,638	72X	88.13%
M029	Normal	93,649,408	79X	88.81%
	Tumor-PB	95,807,367	83X	89.23%
M030	Normal	77,072,181	69X	87.31%
	Tumor-PB	95,518,986	81X	88.85%
M031	Normal	76,749,633	70X	87.84%
	Tumor-PB	88,140,720	79X	88.84%
	Tumor-LN	82,777,634	75X	88.59%
JEKO	Cell line	87,278,089	64X	86.7%
MAVER-1	Cell line	97,178,008	87X	88.6%
MINO	Cell line	84,337,209	52X	86.1%
REC-1	Cell line	90,662,693	77X	88.3%
JVM-2	Cell line	86,788,244	77X	88.4%
Z138	Cell line	117,046,791	85X	89.1%

*These samples were obtained 3.2 (M002) and 3.5 (M003) years after diagnosis.

Table S7. Breakpoints of t(11;14)(q13;q32) translocation by WGS according to the mutational status of *IGHV* gene and SOX11 expression.

Case	Breakpoint chr 14	Breakpoint chr 11	SOX11	% *IGHV* identity	*IGHV*	*IGHD*	*IGHJ*
M001	106329438	69452394	positive	98.80	*IGHV3-21*	*IGHD3-9*	*IGHJ3*
M002	106330070	69440168	positive	99.55	*IGHV4-34*	*IGHD2-15*	*IGHJ6*
M003	106329444	69355770	negative	93.72	*IGHV3-23*	*IGHD3-16*	*IGHJ4*
M004	106329465	69346208	negative	96.99	*IGHV1-8*	*IGHD2-2*	*IGHJ5*

Table S8. Foci of hypermutations or kataegis in three of the four MCL cases analyzed by WGS.

Case	Chromosome	Start	No. mutations	Genes
M002	9	21482492	5	*MIR31HG*
M002	9	22296196	6	-
M003	4	25809285	7	*SEL1L3*
M003	7	52167851	6	-
M003	11	69453595	14	*CCND1*
M003*	4	25809285	7	*SEL1L3*
M003*	7	52167851	6	-
M003*	11	69453595	14	*CCND1*
M004	11	69455892	17	*CCND1*
M004	13	56648266	5	-

The foci of hypermutations in the three immnunoglobulin genes were excluded from the table.
* Sequential sample of patient M003 obtained 3.5 years after diagnosis.

Table S9. MCL mutations identified by WES and Sanger sequencing.

Gene	Case	Exon	Mutation	Total frequency	Frequency of mutations in SOX11+ MCL	Frequency of mutations in SOX11- MCL	Frequency of mutations in *IGHV*-U MCL	Frequency of mutations in *IGHV*-M MCL
ATM	M006	50	p.Q1448A	41.4% (12/29)	54.5% (12/22)*	0/7*	50% (8/16)	25% (3/12)
ATM	M008	8; 56	p.I323V; p.Q2730R					
ATM	M010	63	p.R3008C					
ATM	M012	51	p.R2526S					
ATM	M013	50	p.Y2437S					
ATM	M014	56	p.V2727A					
ATM	M020	39	p.E1959K					
ATM	M022	43; 49	p.W2104*; p.L2427L					
ATM	M024	47	p.A2308T					
ATM	M025	47; 55	p. Q2297*; p.G2694K					
ATM	M030	7; 11	p.R248Q; p.T593fs*20;					
ATM	M031	32; 50	p.R.1618*; p.S2489F					
CCND1	M002	1	p.C47S	34.5% (10/29)	18.2% (4/22)†	6/7 (85.7%)†	18.7% (3/16)‡	58.3% (7/12)‡
CCND1	M003, M011	1	p.Y44S					
CCND1	M004	1	p.Y44Q					
CCND1	M009	1	p.Y44D					
CCND1	M015	1	p.Y44D					
CCND1	M018	1	p.C47S					
CCND1	M022	5	p.V290G					
CCND1	M021	1	p.K46E					
CCND1	M027	1	p.V42E; p.S41T					
MLL2	M002	49	p.A5272P	13.8% (4/29)	18.2% (4/22)	0/7	12.5% (2/16)	16.6% (2/12)
MLL2	M012	33	p.R2771*					
MLL2	M024	21	p.D1724fs*7					
MLL2	M030	39	p.Q3604*					
MLL2	JEKO-1	48	p.R5225C					
MLL2	JVM-2	34	p.S2839*					
WHSC1	M022, M023, M034, M162, M198, M200, M209	18	p.E1099K	10% (13/130)	14.6% (12/82)§	0/31§	14% (11/80)	2.8% (1/35)
WHSC1	M008, M029, M088, M129, M199, M214	19	p.T1150A					

BIRC3	M009	9	p.Q552*	6.4% (11/173)	7.3% (7/95)	7.1% (2/28)	9.2% (9/97)	2.9% (1/34)
BIRC3	M014	9	p.C560Y					
BIRC3	M019	9	Splice site					
BIRC3	M073	9	p.R550*					
BIRC3	M079	9	p.L575V					
BIRC3	M095	9	p.K563*					
BIRC3	M104	9	p.R591fs*1					
BIRC3	M164	9	Large insertion					
BIRC3	M179	9	p.T556fs*11					
BIRC3	M212	9	p.R600G					
BIRC3	M221	9	p.C557G					
NOTCH2	M029, M124, M200, M237	34	p.R2400*	5.2% (9/172)	6.5% (6/93)	3.4% (1/29)	6.3% (6/95)	5.7% (2/35)
NOTCH2	M053	34	p.Q2360*					
NOTCH2	M093	34	p.H2293fs*2					
NOTCH2	M105	34	p.K2292fs*20					
NOTCH2	M128	34	p.S2391fs*2					
NOTCH2	M190	34	p.Q2285*					
NOTCH1	M074, M082, M105, M107, M164, M193	34	p.P2515fs*4	4.6% (8/172)	5.3% (5/95)	0/27	7.4% (7/95)	2.8% (1/35)
NOTCH1	M085	34	p.V2504fs*3					
NOTCH1	M096	34	p.G2281fs*72					
NOTCH1	MINO	34	p.Q2487*					
NOTCH1	REC-1	34	p.H2428fs*7					
MEF2B	M012, M013, M034, M099, M122, M224	2	p.K23R	3.2% (6/187)	5% (5/100)	2.7% (1/36)	4% (4/102)	4.6% (2/43)
MEF2B	REC-1	2	p.N49S					
TLR2	M003	1	p.D327V	1.2% (2/171)	0/94	6.8% (2/29)	0/96	5.7% (2/35)
TLR2	M021	1	p.Y298S					

Data from whole-exome sequencing in 29 primary tumors and from Sanger sequencing in 172 MCL cases from the validation series. Mutations of these genes in the 9 cell lines studied are indicated but not considered in the frequency values. *IGHV*-M: mutated *IGHV* gene; *IGHV*-U: unmutated *IGHV* gene.
**P*-value=0.023;†*P*-value=0.003; ‡*P*-value= 0.05; and § *P*-value= 0.034.

Table S10. Regions of copy number and CNN-LOH identified in the 29 MCL from the exome series (Hg19).

Sample	Chromosome	Start	End	Aberration Type	Segment size (Kb)	Band	No. Probes
M001-PB							
M001-PB	chr3	118228538	197962430	Gain	79791	q13.32 - q29	50174
M001-PB	chr5	10001	669793	Gain	723	p15.33	307
M001-PB	chr5	1131169	1633450	Amplification	502	p15.33	308
M001-PB	chr5	4336320	12109540	Gain	7773	p15.33 - p15.2	6831
M001-PB	chr5	49459042	49930748	Gain	472	q11.1	182
M001-PB	chr6	75087596	78517856	Gain	3430	q13 - q14.1	2202
M001-PB	chr6	79448530	80355169	Gain	907	q14.1	547
M001-PB	chr6	80737260	171055067	Loss	90106	q14.1 - q27	60076
M001-PB	chr8	40642	26893704	Loss	26919	p23.3 - p21.2	24256
M001-PB	chr10	110027	21948498	Loss	21888	p15.3 - p12.31	18275
M001-PB	chr10	22602820	22705943	Gain	103	p12.31	52
M001-PB	chr10	22982715	26122776	Gain	3140	p12.2 - p12.1	2207
M001-PB	chr10	26709813	27920184	Gain	1210	p12.1	823
M001-PB	chr10	31874561	35324983	Gain	3450	p11.22 - p11.21	2387
M001-PB	chr15	40586080	49772806	Loss	9187	q15.1 - q21.1	5157
M001-PB	chr15	53907813	59453515	Loss	5546	q21.3 - q22.2	3854
M001-PB	chr15	77296172	78597748	Loss	1302	q24.3 - q25.1	688
M001-PB	chr15	85550484	102453674	Loss	16920	q25.3 - q26.3	13142
M001-PB	chr18	10001	921791	Loss	912	p11.32	687
M001-PB	chr18	953961	77931412	Gain	75088	p11.32 - q23	51306
M001-PB	chr20	35716451	45537371	Loss	9821	q11.23 - q13.12	7015
M001-PB	chr21	36205735	38336700	Loss	2131	q22.12 - q22.13	1621
M001-PB	chr21	42131041	48119895	Loss	5891	q22.2 - q22.3	4068
M001-LN							
M001-LN	Same alterations than M001-PB						
M002-Tonsil							
M002-Tonsil	chr1	92441110	112610039	Loss	20198	p22.1 - p13.2	12982
M002-Tonsil	chr7	10238	159128663	Gain	158821	p22.3 - q36.3	100943
M002-Tonsil	chr9	19944309	21447292	Loss	1503	p21.3	1221
M002-Tonsil	chr9	21486917	22258314	Homozygous Loss	771	p21.3	589
M002-Tonsil	chr9	22263398	23,132,697	Loss	869	p21.3	578
M002-Tonsil	chr9	70459309	119909343	Loss	49250	q12 - q33.1	36113
M002-Tonsil	chr12	7266783	16848153	Loss	9581	p13.31 - p12.3	6459
M002-Tonsil	chr13	50488933	91937630	Loss	41349	q14.3 - q31.3	26247
M002-Tonsil	chr13	91959820	92907213	Amplification	947	q31.3	649

M002-Tonsil	chr13	92907213	96843698	Loss	3936	q31.3 - q32.1	2778
M002-Tonsil	chr13	96843698	98643681	Homozygous Loss	1800	q32.1 - q32.2	1137
M002-Tonsil	chr13	98643681	115109878	Loss	16701	q32.2 - q34	12433
M002-PB*							
M002-PB*	chr1	92719701	116092430	Loss	23402	p22.1 - p13.2	15112
M002-PB*	chr4	163826497	174889279	Gain	11080	q32.2 - q34.1	6991
M002-PB*	chr4	175912522	191029082	Gain	15124	q34.1 - q35.2	10757
M002-PB*	chr6	127627822	168076129	Loss	40149	q22.33 - q27	28336
M002-PB*	chr6	168090016	170940576	Homozygous Loss	2950	q27	2003
M002-PB*	chr8	111196706	111377912	Loss	181	q23.2	84
M002-PB*	chr8	112727257	113735049	Gain	1008	q23.3	556
M002-PB*	chr9	70459309	119909343	Loss	49250	q13 - q33.1	35328
M002-PB*	chr11	111162358	115328488	Loss	4166	q23.1 - q23.2	2943
M002-PB*	chr12	7266783	16848153	Loss	9581	p13.31 - p12.3	6459
M002-PB*	chr13	50488933	115109878	Loss	64820	q14.3 - q34	43286
M002-PB*	chr17	0	18565792	CNN-LOH	18507	p13.3 - p11.2	11878
M003-PB							
M003-PB	chr17	0	22263006	Loss	22200	p13.3 - q11.1	13449
M003-PB*							
M003-PB*	chr3	67963843	68626981	Loss	663	p14.1	462
M003-PB*	chr3	68740108	197962430	Gain	130679	p14.1 - q29	78692
M003-PB*	chr4	70508182	70747314	Loss	239	q13.3	137
M003-PB*	chr4	70747315	71810114	Gain	1247	q13.3	631
M003-PB*	chr4	71810114	74531882	Loss	2722	q13.3	1598
M003-PB*	chr4	114329605	115160104	Loss	831	q26	583
M003-PB*	chr4	115183202	115730796	Gain	548	q26	350
M003-PB*	chr4	115730796	116036778	Loss	306	q26	195
M003-PB*	chr4	116036778	126765787	Gain	10726	q26 - q28.1	6556
M003-PB*	chr4	190778400	191029082	Gain	258	q35.2	70
M003-PB*	chr8	66646199	146304022	Gain	79466	q13.1 - q24.3	51319
M003-PB*	chr12	145739	8982647	Gain	8874	p13.33 - p13.31	6014
M003-PB*	chr12	8982660	9192134	Loss	209	p13.31	141
M003-PB*	chr12	9193286	9275102	Gain	81	p13.31	54
M003-PB*	chr12	9275103	15622186	Loss	6347	p13.31 - p12.3	4607
M003-PB*	chr12	15622187	15890740	Gain	269	p12.3	144
M003-PB*	chr12	15890740	17368844	Loss	1478	p12.3	937
M003-PB*	chr12	46243873	47284789	Loss	1041	q12 - q13.11	590
M003-PB*	chr12	47304835	79376245	Gain	32309	q13.11 - q21.2	20398
M003-PB*	chr12	79378845	80533230	Loss	1154	q21.2 - q21.31	675
M003-PB*	chr17	0	22263006	Loss	22200	p13.3 - q11.1	13449
M004-PB							
M004-PB	chr1	179776977	249233096	Loss	69206	q25.2 - q44	48500

M004-PB	chr8	10001	43838887	Loss	43974	p23.3 - p11.1	34658
M004-PB	chr13	50417633	51459447	Loss	1042	q14.3	653
M004-PB	chr16	79059660	79608761	Gain	549	q23.1	656
M004-PB	chr17	0	22263006	Loss	22200	p13.3 - q11.1	13449
M004-PB	chr18	64736967	65074844	Gain	338	q22.1	260
M006-PB							
M006-PB	chr1	22275416	32683292	Loss	10308	p36.12 - p35.1	5650
M006-PB	chr1	152746697	174782872	Loss	22036	q21.3 - q25.1	15285
M006-PB	chr4	62171342	94286034	Loss	32651	q13.1 - q22.2	19910
M006-PB	chr5	10000	1348012	Gain	1401	p15.33	641
M006-PB	chr8	10001	36140133	Loss	36260	p23.3 - p12	30253
M006-PB	chr8	36172446	146117505	Gain	109796	p12 - q24.3	67822
M006-PB	chr10	60001	572671	Loss	563	p15.3	303
M006-PB	chr10	609825	17251652	Loss	16692	p15.3 - p13	14583
M006-PB	chr10	17272707	34661687	Gain	17389	p12.33 - p11.21	12446
M006-PB	chr11	104857579	112252510	Loss	7395	q22.3 - q23.1	4803
M006-PB	chr12	145739	2419151	Gain	2289	p13.33	1468
M006-PB	chr12	3311443	6257833	Gain	2946	p13.32 - p13.31	2601
M006-PB	chr12	7241152	9875493	Gain	2639	p13.31	1400
M006-PB	chr12	10417982	17114750	Loss	6697	p13.2 - p12.3	4829
M006-PB	chr12	17119643	22895822	Amplification	5776	p12.3 - p12.1	3792
M006-PB	chr12	22954573	25370445	Loss	2416	p12.1	1836
M006-PB	chr17	42958765	81060000	Gain	38460	q21.31 - q25.3	23053
M006-PB	chr18	54852270	78016181	Gain	23114	q21.31 - q23	17293
M006-PB	chr21	14354777	24404829	Loss	10050	q11.2 - q21.2	7091
M006-PB	chr21	27155370	33211849	Loss	6056	q21.3 - q22.11	4579
M006-PB	chr12	17697264	22854564	CNN-LOH	5157	p12.3 - p12.1	1617
M007-Colon							
M007-Colon	chr9	10002	141153431	Loss	140273	p24.3 - q34.3	82094
M007-Colon	chr1	72445714	117234591	Loss	44818	p31.1 - p13.1	29553
M007-Colon	chr11	93530173	117676671	Loss	24012	q21 - q23.3	17356
M008-PB							
M008-PB	chr1	62367186	109308733	Loss	46970	p31.3 - p13.3	31088
M008-PB	chr3	124624944	197962430	Gain	73394	q21.2 - q29	46269
M008-PB	chr4	181756054	181963383	Loss	207	q34.3	148
M008-PB	chr10	60000	39088250	Gain	39128	p15.3 - p11.1	29962
M008-PB	chr12	9354560	13902910	Loss	4548	p13.31 - p13.1	3483
M008-PB	chr17	0	9423484	Loss	9364	p13.3 - p13.1	5530
M008-PB	chr22	16619782	51244566	Loss	34692	q11.1 - q13.33	24376
M009-PB							
M009-PB	No alterations						
M009-PB*							

M009-PB*	No alterations						
M010-PB							
M010-PB	chr3	129233155	197962430	Gain	68786	q21.3 - q29	43476
M010-PB	chr4	10001	11783917	Gain	11393	p16.3 - p15.33	7525
M010-PB	chr6	84360191	94020647	Gain	9660	q14.2 - q16.1	6361
M010-PB	chr6	94056956	171014636	Loss	76743	q16.1 - q27	51328
M010-PB	chr8	66827451	146304022	Gain	79285	q13.1 - q24.3	51242
M010-PB	chr10	60000	1720790	Loss	1711	p15.3	1159
M010-PB	chr10	1894011	21061431	Loss	19217	p15.3 - p12.1	16395
M010-PB	chr10	21061431	25691351	Amplification	4629	p12.31-p12.1	2945
M010-PB	chr10	25691351	26738039	Loss	1047	p12.1	812
M010-PB	chr10	26740330	34256021	Amplification	7516	p12.1 - p11.22	5587
M010-PB	chr10	34273216	34393099	Loss	120	p11.22	79
M010-PB	chr10	34396074	43742726	Amplification	8627	p11.22 - q11.21	3504
M010-PB	chr11	90462909	114353338	Loss	23756	q14.3 - q23.2	17159
M010-PB	chr11	122800174	122911190	Gain	111	q24.1	99
M010-PB	chr11	127804127	131062373	Gain	3258	q24.2 - q25	2517
M010-PB	chr11	132937952	134128707	Gain	1191	q25	882
M010-PB	chr12	38265653	52271159	Loss	14006	q12 - q13.13	8357
M010-PB	chr12	52334865	126938225	Gain	74883	q13.13 - q24.32	49083
M010-PB	chr13	19040087	30246342	Gain	11206	q11 - q12.3	8211
M010-PB	chr13	30262179	30367290	Loss	105	q12.3	66
M010-PB	chr13	30808973	115109878	Loss	84436	q12.3 - q34	57308
M010-PB	chr15	22574003	27084903	Gain	4561	q11.2 - q12	2852
M010-PB	chr15	27088958	48451277	Loss	21599	q12 - q21.1	13330
M010-PB	chr15	48480278	59178707	Gain	10698	q21.1 - q22.1	7211
M010-PB	chr15	59178707	61016476	Loss	1838	q22.1 - q22.2	1322
M010-PB	chr15	61056591	86197895	Gain	25155	q22.2 - q25.3	15444
M010-PB	chr15	86243890	102521392	Loss	16294	q25.3 - q26.3	12712
M010-PB	chr16	69881232	90294753	Loss	20389	q22.1 - q24.3	17120
M010-PB	chr18	10001	78016181	Gain	76117	p11.32 - q23	52074
M010-PB	chr22	23222285	34580262	Loss	11358	q11.22 - q12.3	8690
M010-PB	chr22	34749460	35414802	Loss	665	q12.3	657
M010-PB	chr22	50438629	51244566	Loss	911	q13.33	366
M010-LN							
M010-LN	Same alterations than M010-PB						
M011-LN							
M011-LN	chr2	59485760	70962728	Gain	11477	p16.1 - p13.3	7520
M011-LN	chr7	10238	55150251	Gain	55118	p22.3 - p11.2	40167
M011-LN	chr13	45439558	115085462	Loss	69766	q14.12 - q34	46598
M011-LN	chr20	24956036	62965520	CNN-LOH	37532	p11.21 - q13.33	11906
M012-LN							

M012-LN	chr1	66392830	114699474	Loss	48336	p31.3 - p13.2	31835
M012-LN	chr11	75958707	116614665	Loss	40484	q13.5 - q23.3	28896
M012-LN	chr11	116623872	134926481	Gain	18303	q23.3 - q25	13898
M012-LN	chr11	69314155	75846643	Gain	6501	q13.2 - q13.5	3599
M012-LN	chr14	27215007	107289540	CNN-LOH	80084	q12 - q32.33	25533
M013-LN							
M013-LN	chr11	94439147	116616201	Loss	22043	q21 - q23.3	15975
M013-LN	chr19	60000	20771689	Loss	20564	p13.3 - p12	9412
M014-LN							
M014-LN	chr1	26345580	27980718	Loss	1635	p36.11 - p35.3	669
M014-LN	chr1	48813881	109293627	Loss	60509	p33 - p13.3	40223
M014-LN	chr4	10001	34068651	Loss	33745	p16.3 - p15.1	23016
M014-LN	chr4	66024549	66580419	Loss	556	q13.1	392
M014-LN	chr4	66801389	190965327	Gain	124718	q13.2 - q35.2	78347
M014-LN	chr6	60000	17711354	Gain	17819	p25.3 - p22.3	14176
M014-LN	chr7	97333932	105169119	Loss	7784	q21.3 - q22.2	3971
M014-LN	chr7	133754314	142048195	Loss	8447	q33 - q34	5773
M014-LN	chr9	118631656	123768423	Gain	5137	q33.1 - q33.2	4254
M014-LN	chr11	94944462	115392644	Loss	20314	q21 - q23.2	14596
M014-LN	chr12	51745585	133690335	Gain	82169	q13.13 - q24.33	54714
M014-LN	chr13	30039657	114996266	Loss	85077	q12.3 - q34	57860
M015-PB							
M015-PB	chr4	169755354	191029082	CNN-LOH	21281	q32.3 - q35.2	7187
M016-PB							
M016-PB	No alterations						
M016-Spleen							
M016-Spleen	No alterations						
M018-PB							
M018-PB	chr1	222856225	249233096	Loss	26327	q41 - q44	18772
M018-PB	chr3	60000	3274288	Loss	3249	p26.3	2954
M018-PB	chr3	3281997	10038512	Gain	6757	p26.3 - p25.3	5841
M018-PB	chr3	10081168	48127305	Loss	38046	p25.3 - p21.31	25820
M018-PB	chr3	53252950	81520610	Loss	28375	p21.1 - p12.3	20707
M018-PB	chr3	81537706	89190218	Gain	7653	p12.3 - p11.2	4186
M018-PB	chr3	89190551	90327821	Loss	1137	p11.2 - p11.1	652
M018-PB	chr3	93504854	197962430	Gain	104541	q11.2 - q29	65301
M018-PB	chr9	119303209	119406431	Gain	103	q33.1	90
M018-PB	chr11	76524661	107071976	Loss	30375	q13.5 - q22.3	21827
M018-PB	chr11	114337621	118753954	Gain	4416	q23.2 - q23.3	3277
M018-PB	chr11	118791727	134946516	Loss	16155	q23.3 - q25	12388
M018-PB	chr13	52192230	57333147	Loss	5141	q14.3 - q21.1	2881
M018-PB	chr13	57335168	67889300	Gain	10554	q21.1 - q21.32	6515
M018-PB	chr13	67906464	69569939	Loss	1663	q21.32 - q21.33	1033

M018-PB	chr13	69578476	75074801	Gain	5496	q21.33 - q22.1	3883
M018-PB	chr13	75102448	78141952	Loss	3040	q22.1 - q22.3	2183
M018-PB	chr13	78142711	85388208	Gain	7245	q22.3 - q31.1	4712
M018-PB	chr13	85402516	89187470	Loss	3685	q31.1 - q31.2	2188
M018-PB	chr13	89199840	100438134	Gain	11238	q31.2 - q32.3	7618
M018-PB	chr13	100459456	115109878	Loss	14886	q32.3 - q34	11092
M018-PB	chr14	20427715	52024134	Loss	31596	q11.2 - q22.1	20340
M018-PB	chr14	61274088	64178171	Loss	2904	q23.1 - q23.2	1970
M018-PB	chr17	0	22263006	Loss	22190	p13.3 - p11.1	13449
M018-PB	chr17	25343462	81060000	Gain	56407	q11.1 - q25.3	33117
M018-PB	chr18	18510899	29689338	Loss	11843	q11.1 - q12.1	7012
M018-PB	chr18	31206556	42356111	Loss	11150	q12.1 - q12.3	7307
M018-PB	chr20	35902804	39794241	Loss	3891	q11.23 - q12	2707
M018-PB	chr22	38519181	39125849	Loss	607	q13.1	342
M018-PB	chr22	39743177	40317912	Loss	575	q13.1	294
M018-PB	chr22	41870544	42878175	Loss	1008	q13.2	554
M019-PB							
M019-PB	chr1	49565292	111345628	Loss	61809	p33 - p13.3	41058
M019-PB	chr1	111355396	115738454	Gain	4383	p13.3 - p13.2	3118
M019-PB	chr1	115749096	119924040	Loss	4175	p13.2 - p12	2738
M019-PB	chr3	121590268	197962430	Gain	76429	q13.33 - q29	48286
M019-PB	chr6	131180953	171055067	Loss	39677	q23.1 - q27	27912
M019-PB	chr8	85871765	146304022	Gain	60241	q21.2 - q24.3	39484
M019-PB	chr11	77464144	116968043	Loss	39331	q14.1 - q23.3	28250
M019-PB	chr12	145740	14042668	Loss	13934	p13.33 - p13.1	9840
M019-PB	chr12	14043172	44802351	Gain	29154	p13.1 - q12	18745
M019-PB	chr12	44904486	51138863	Loss	6234	q12 - q13.13	3487
M019-PB	chr12	51230714	133779461	Gain	82786	q13.13 - q24.33	55044
M019-PB	chr13	19092836	115070463	Loss	96098	q11 - q34	65937
M019-PB	chr15	47040178	102521392	Gain	55511	q21.1 - q26.3	37785
M020-PB							
M020-PB	chr1	92734376	106260827	Loss	13555	p22.1 - p21.1	8338
M020-PB	chr1	202457542	204671311	Gain	2214	q32.1	1572
M020-PB	chr2	3434730	3655068	Gain	219	p25.3	98
M020-PB	chr5	10000	43879590	Gain	43915	p15.33 - p12	30575
M020-PB	chr7	135133619	139078666	Loss	3945	q33 - q34	2545
M020-PB	chr7	139113500	145351269	Gain	6218	q34 - q35	4176
M020-PB	chr10	111558	21828550	Loss	21767	p15.3 - p12.31	18228
M020-PB	chr10	21828550	23356686	Gain	1528	p12.31 - p12.2	827
M020-PB	chr11	69356340	69902170	Gain	514	q13.2 - q13.3	316
M020-PB	chr13	19061608	115109878	Loss	96183	q11 - q34	65957
M020-PB	chr18	59621511	61814015	Gain	2193	q21.33 - q22.1	1611

M020-PB	chr19	18119733	19067475	Loss	948	p13.11	358
M021-PB							
M021-PB	chr1	49824939	49960149	Loss	135	p33	61
M021-PB	chr4	146478623	146609240	Gain	131	q31.22	77
M021-PB	chr16	3602914	3813801	Loss	211	p13.3	96
M022-LN							
M022-LN	chr1	10001	109824127	Loss	109626	p36.33 - p13.3	68270
M022-LN	chr3	126806952	197962430	Gain	71212	q21.3 - q29	44906
M022-LN	chr4	39335668	40113249	Loss	778	p14	352
M022-LN	chr6	153821992	154203684	Gain	382	q25.2	292
M022-LN	chr9	10001	21584421	Loss	21574	p24.3 - p21.3	19801
M022-LN	chr9	21626584	22352655	Homozygous Loss	726	p21.3	522
M022-LN	chr9	22361470	34310915	Loss	11949	p21.3 - p13.3	8830
M022-LN	chr12	145739	133779461	Gain	132350	p13.33 - q24.33	87226
M022-LN	chr13	44251262	84313839	Loss	40063	q14.11 - q31.1	25784
M022-LN	chr13	84442270	115109878	Gain	30803	q31.1 - q34	21533
M022-LN	chr15	20057581	49091001	Loss	28561	q11.1 - q21.1	17155
M022-LN	chr16	60001	35223009	Gain	35081	p13.3 - p11.1	21529
M022-LN	chr16	46385801	90294753	Loss	43889	q11.2 - q24.3	32649
M022-LN	chr18	34401	44984531	Gain	43214	p11.32 - q21.1	27874
M022-LN	chr18	45014851	78016181	Amplification	32848	q21.1 - q23	24176
M022-LN	chr19	60000	24438612	Loss	24230	p13.3 - p12	11621
M022-LN	chr19	35762331	59114839	Gain	23357	q13.12 - q13.43	13010
M022-LN	chr20	60000	25061561	Gain	25010	p13 - p11.21	20057
M022-LN	chr20	35091046	62949607	Loss	27896	q11.23 - q13.33	20359
M022-LN	chr22	16055171	21462521	Gain	5357	q11.1 - q11.21	2978
M022-LN	chr22	24961984	51244566	Loss	26399	q11.23 - q13.33	19283
M022-LN	chr13	84412574	115109878	CNN-LOH	30832	q31.1 - q34	11728
M022-LN	chr15	48682937	102521392	CNN-LOH	53869	q21.1 - q26.3	18245
M023-PB							
M023-PB	chr3	60000	197962430	Gain	199502	p26.3 - q29	127688
M023-PB	chr5	122961804	125425537	Loss	2464	q23.2	1787
M023-PB	chr6	103942071	143559709	Loss	39553	q16.3 - q24.2	25442
M023-PB	chr10	10936883	12321770	Loss	1385	p14 - p13	1034
M023-PB	chr12	11803438	11983144	Loss	180	p13.2	263
M023-LN							
M023-LN	chr1	81993939	115117360	Loss	33152	p31.1 - p13.2	21769
M023-LN	chr3	60000	197962430	Gain	199502	p26.3 - q29	127688
M023-LN	chr5	131025868	132118371	Loss	1093	q31.1	636
M023-LN	chr5	133725149	133947166	Loss	222	q31.1	126

M023-LN	chr6	103942071	143559709	Loss	39553	q16.3 - q24.2	25442
M023-LN	chr8	38408736	39086752	Loss	678	p11.23	334
M023-LN	chr3	170169054	181957056	CNN-LOH	11788	q26.2 - q26.33	3368
M024-LN							
M024-LN	chr7	10238	23565889	Gain	23532	p22.3 - p15.3	17319
M024-LN	chr11	92920606	116864526	Loss	23809	q21 - q23.3	17224
M024-LN	chr13	112183398	115109878	Loss	3162	q34	1395
M024-LN	chr19	60000	16388502	CNN-LOH	16213	p13.3-p13.11	2817
M025-LN							
M025-LN	chr1	84222669	114281587	Loss	30088	p31.1 - p13.2	19739
M025-LN	chr4	5337073	24205745	Gain	18427	p16.1 - p15.2	13836
M025-LN	chr5	10000	9524825	Gain	9578	p15.33 - p15.2	7963
M025-LN	chr6	128109231	160774143	Loss	32543	q22.33 - q25.3	22381
M025-LN	chr6	160802024	171055067	Gain	10178	q25.3 - q27	7651
M025-LN	chr8	131948999	140601876	Gain	8653	q24.22 - q24.3	7235
M025-LN	chr9	70462156	141153431	Loss	70571	q12 - q34.3	49278
M026-PB							
M026-PB	chr3	24864378	48804598	Loss	23940	p24.2 - p21.31	15834
M026-PB	chr5	10000	39498244	Gain	39534	p15.33 - p13.1	27946
M026-PB	chr6	24443851	26369485	Loss	1926	p22.2 - p22.1	1360
M026-PB	chr8	79114280	146304022	Gain	66998	q21.12 - q24.3	43470
M026-PB	chr9	70626756	141153431	Loss	70407	q12 - q34.3	49278
M026-PB	chr11	85993139	116616201	Loss	30451	q14.2 - q23.3	21826
M026-PB	chr13	19107653	41614720	Loss	22507	q11 - q14.11	16618
M026-PB	chr13	46887803	73446141	Loss	26558	q14.12 - q22.1	16585
M026-PB	chr13	73703365	85278428	Gain	11575	q22.1 - q31.1	7960
M026-PB	chr13	87774121	89561029	Loss	1787	q31.2	994
M026-PB	chr13	90076715	92019703	Loss	1943	q31.3	1268
M026-PB	chr13	93673889	115109878	Gain	21671	q31.3 - q34	15826
M026-PB	chr17	7257735	8340943	Loss	1083	p13.1	519
M026-LN							
M026-LN	Same alterations than M026-PB						
M027-PB							
M027-PB	chr17	0	21495013	Loss	21436	p13.3 - p11.2	13190
M028-PB							
M028-PB	chr1	10001	25897102	Gain	25770	p36.33 - p36.11	14738
M028-PB	chr1	73914793	104530894	Loss	30645	p31.1 - p21.1	20009
M028-PB	chr3	9365508	9511991	Amplification	146	p25.3	85
M028-PB	chr3	9511991	16213170	Gain	6701	p25.3 - p24.3	4699
M028-PB	chr3	16732967	19824062	Amplification	3091	p24.3	1684

M028-PB	chr3	19869590	25101200	Gain	5232	p24.3 - p24.2	3864
M028-PB	chr3	25101833	27954144	Amplification	2852	p24.2 - p24.1	2175
M028-PB	chr3	27959843	31149972	Gain	3190	p24.1 - p23	2438
M028-PB	chr4	127044487	177997173	Gain	50970	q28.1 - q34.3	31669
M028-PB	chr4	178016782	179189691	Amplification	1173	q34.3	852
M028-PB	chr4	179194413	191029082	Gain	11842	q34.3 - q35.2	8592
M028-PB	chr7	138787299	142048195	Amplification	3367	q34	2244
M028-PB	chr8	128036993	129358220	Gain	1321	q24.21	1038
M028-PB	chr9	10001	38733320	Loss	38723	p24.3 - p13.1	32014
M028-PB	chr10	60000	16967637	Gain	17008	p15.3 - p13	14651
M028-PB	chr11	69022446	134946516	Loss	65673	q13.2 - q25	46619
M028-PB	chr12	49064967	51630527	Loss	2566	q13.11 - q13.13	1201
M028-PB	chr13	19020000	48893060	Loss	29893	q11 - q14.2	21669
M028-PB	chr13	48899012	49143747	Homozygous Loss	245	q14.2	241
M028-PB	chr13	49170671	115087164	Loss	66037	q14.2 - q34	44006
M028-PB	chr18	23101688	78016181	Gain	54761	q11.2 - q23	38626
M028-PB	chr19	60000	17970312	Loss	17795	p13.3 - p13.11	8066
M028-PB	chr19	52079455	55378682	Gain	3299	q13.33 - q13.42	2248
M028-PB	chr9	70620211	141153431	CNN-LOH	70413	q12 - q34.3	24392
M029-PB							
M029-PB	chr2	231047501	231384877	Loss	337	q37.1	204
M029-PB	chr3	127274309	175125742	Gain	47851	q21.3 - q26.31	30039
M029-PB	chr3	175484095	197910502	Gain	22428	q26.31 - q29	14307
M029-PB	chr6	31135152	31957099	Loss	822	p21.33 - p21.32	423
M029-PB	chr9	82641048	105321734	Loss	22531	q21.31 - q31.1	15834
M029-PB	chr13	86660977	91685755	Gain	4925	q31.1 - q31.3	2885
M029-PB	chr13	91685755	93783197	Amplification	2097	q31.3	1446
M029-PB	chr13	93783197	115109878	Loss	21562	q31.3 - q34	15742
M029-PB	chr19	13529277	15220189	Loss	1691	p13.13 - p13.12	877
M029-PB	chr19	38556539	59114839	Gain	20563	q13.13 - q13.43	11525
M029-PB	chr6	60000	29914882	CNN-LOH	30023	p25.3 - p21.33	12291
M029-PB	chr17	0	12471864	CNN-LOH	12412	p13.3-p12	3813
M030-PB							
M030-PB	chr1	73659352	117864819	Loss	44234	p31.1 - p12	29241
M030-PB	chr3	104168982	197680244	Gain	93513	q13.11 - q29	59214
M030-PB	chr11	69325821	70432310	Gain	1075	q13.2 - q13.3	620
M030-PB	chr9	10001	36046396	CNN-LOH	36036	p24.3 - p13.3	16071
M030-PB	chr22	18361113	51244566	CNN-LOH	32950	q11.21 - q13.33	11030
M031-PB							

M031-PB	chr1	63746213	105645259	Loss	41928	p31.3 - p21.1	27609
M031-PB	chr2	25380974	25847971	Loss	467	p23.3	233
M031-PB	chr2	42924187	43983285	Loss	1059	p21	748
M031-PB	chr2	111441265	113308818	Loss	1868	q13	940
M031-PB	chr6	55789771	70012642	Loss	14172	p12.1 - q13	6504
M031-PB	chr6	72722361	76927295	Amplification	4205	q13 - q14.1	2670
M031-PB	chr6	76932144	110226668	Loss	33344	q14.1 - q21	21576
M031-PB	chr8	98478588	128740542	Gain	30262	q22.1 - q24.21	19530
M031-PB	chr8	129181703	146304022	Gain	17024	q24.21 - q24.3	11959
M031-PB	chr9	10001	5850933	Loss	5841	p24.3 - p24.1	5978
M031-PB	chr9	5864467	7135848	Amplification	1271	p24.1	1007
M031-PB	chr9	7137335	11690218	Gain	4553	p24.1 - p23	4378
M031-PB	chr9	11695349	21076512	Loss	9381	p23 - p21.3	8004
M031-PB	chr9	21077639	21997496	Homozygous Loss	920	p21.3	698
M031-PB	chr9	22020740	38812793	Loss	16792	p21.3 - p13.1	11932
M031-PB	chr10	86267	12620392	Loss	12584	p15.3 - p13	10860
M031-PB	chr13	19045628	20544541	Gain	1499	q11 - q12.11	796
M031-PB	chr13	20608233	90919918	Loss	70212	q12.11 - q31.3	47489
M031-PB	chr13	90927968	98524680	Amplification	7597	q31.3 - q32.2	5155
M031-PB	chr13	98536247	115109878	Loss	16799	q32.2 - q34	12476
M031-PB	chr17	74040949	74760783	Loss	720	q25.1 - q25.2	418
M031-LN							
M031-LN	Same alterations than M031-PB						

Abbreviations: CNN-LOH, Copy number neutral loss of heterozygosity; LN, lymph node; PB, Peripheral Blood.
*These samples were obtained 3.2, 3.5 and 5 years after diagnosis, respectively.

Table S11. Recurrently mutated genes identified in the 29 MCL analyzed by WES, based on recurrence, gene size and gene coverage.

Recurrent significant mutated genes (*P*<0.01)				
Gene	**Case**	**No. of mutations**	**No. of mutations**	***P*-value**
*ATM**	M006, M008, M010, M012, M013, M014, M020, M022, M024, M025, M030, M031	17	12	<0.0001
*CCND1**	M002, M003, M004, M009, M011, M015, M018, M021, M022, M027	12	10	<0.0001
*TP53**	M003, M004, M010, M018, M026, M027, M028, M029	9	8	<0.0001
*WHSC1**	M008, M022, M023, M029	4	4	<0.0001
*MLL2**	M002, M012, M024, M030	4	4	0.0007
*BIRC3**	M009, M014, M019	3	3	<0.0001
MEF2B	M012, M013	2	2	0.0001
CHMP4C	M006, M022	2	2	0.0001
LUZP4	M010, M024	2	2	0.0002
RGS4	M007, M029	2	2	0.0002
PDLIM3	M002, M012	2	2	0.0003
KCNC2	M009, M031	2	2	0.0009
SLC17A6	M003, M018	2	2	0.0010
DCP1B	M024. M028	2	2	0.0010
PCSK2	M001, M013	2	2	0.0011
SP140	M025, M028	2	2	0.0014
TLR2	M003, M021	2	2	0.0018
TRPM6	M004, M031	2	2	0.0021
DLGAP2	M007, M014	2	2	0.0023
DNAJC6	M006, M030	2	2	0.0024
TNRC6B	M016, M030	2	2	0.0027
CRYBG3	M014, M030	2	2	0.0030
ABCA3	M002, M006	2	2	0.0061
KIAA1671	M010, M030	2	2	0.0063
ABCC9	M025, M028	2	2	0.0067
Recurrent non-significant mutated genes				
Gene	**Case**	**No. of mutations**	**No. of mutated cases**	***P*-value**
FLNC	M006, M030	2	2	0.0154
UBR5	M006, M023	2	2	0.0198
UNC80	M007, M018	2	2	0.0256
CSMD2	M001, M011	2	2	0.0285
CSMD3	M024, M028	2	2	0.0343
LRP1B	M010, M022	2	2	0.0504
SYNE1	M013, M030	2	2	0.1498
TTN	M002, M003, M028	4	3	0.1610

*Genes present in the Cancer Gene Census, all of them in hematologic neoplasms (http://www.sanger.ac.uk/genetics/CGP/Census/).

Table S12. Significant differentially expressed genes between *WHSC1*-mutated and -unmutated cases.

ProbeSet	Gene symbol	FDR	Fold-change	ProbeSet	Gene symbol	FDR	Fold-change
228831_s_at	*GNG7*	< 1e-07	10.25	**204669_s_at**	*RNF24*	0.00332	0.58
225802_at	*TOP1MT*	0.0181	2.99	**210882_s_at**	*TRO*	0.0164	0.58
204285_s_at	*PMAIP1*	0.00928	2.86	**239162_at**	*DAPK1-IT1*	0.0237	0.57
212311_at	*SEL1L3*	0.00764	2.86	**237105_at**	*LOC100506831*	0.00735	0.57
222735_at	*TMEM38B*	0.0459	2.47	**219451_at**	*MSRB2*	0.0316	0.57
229050_s_at	*SNHG7*	0.0265	1.97	**234929_s_at**	*SPATA7*	0.00182	0.57
226240_at	*TADA2B*	0.00191	1.97	**223475_at**	*CRISPLD1*	0.0059	0.56
218494_s_at	*SLC2A4RG*	0.0181	1.95	**211276_at**	*TCEAL2*	0.00021	0.56
214001_x_at	*RPS10*	0.0338	1.93	**244334_at**	*TRAM1L1*	< 1e-07	0.56
1556389_at	*CNPY3*	0.0275	1.89	**242592_at**	*GPR137C*	0.0349	0.55
204487_s_at	*KCNQ1*	0.0426	1.85	**205899_at**	*CCNA1*	0.0237	0.54
205594_at	*ZNF652*	0.0478	1.8	**242881_x_at**	*LOC100506303*	0.0104	0.54
219305_x_at	*FBXO2*	0.00408	1.67	**242119_at**	*PROX1*	< 1e-07	0.54
223318_s_at	*ALKBH7*	0.0394	1.65	**211602_s_at**	*TRPC1*	0.023	0.54
1558761_a_at	*FAM120AOS*	0.0368	1.61	**202133_at**	*WWTR1*	0.000693	0.54
224912_at	*TTC7A*	0.0365	1.61	**209030_s_at**	*CADM1*	0.0129	0.53
208717_at	*OXA1L*	0.0353	1.56	**219017_at**	*ETNK1*	0.0334	0.53
238659_at	*KIAA0141*	0.0455	1.54	**204627_s_at**	*ITGB3*	0.0317	0.53
217925_s_at	*C6orf106*	0.0241	1.49	**201397_at**	*PHGDH*	0.0308	0.53
209075_s_at	*ISCU*	0.0342	1.48	**203476_at**	*TPBG*	0.000265	0.53
1569868_s_at	*EME2*	0.0326	1.43	**227415_at**	*LOC283508*	0.0104	0.52
224078_at	*HIATL2*	0.0178	1.4	**200906_s_at**	*PALLD*	0.00021	0.52
205354_at	*GAMT*	0.0453	1.38	**225599_s_at**	*C8orf83*	0.00779	0.51
202263_at	*CYB5R1*	0.0199	1.36	**223854_at**	*PCDHB10*	0.0342	0.51
217399_s_at	*FOXO3*	0.0355	1.27	**201928_at**	*PKP4*	0.0344	0.51
213944_x_at	*GNA11*	0.0328	1.26	**227657_at**	*RNF150*	0.000265	0.51
214367_at	*RASGRP2*	0.0322	1.26	**215047_at**	*TRIM58*	0.0261	0.51
229188_s_at	*ZNRF2*	0.0308	1.26	**230175_s_at**	*DCBLD2*	0.00451	0.5
1560994_x_at	*LOC400590*	0.0199	1.25	**239108_at**	*FAR2*	0.00543	0.5
216119_s_at	*SPEF1*	0.0322	1.25	**205889_s_at**	*JAKMIP2*	0.000571	0.5
208929_x_at	*RPL13*	0.0417	1.24	**219510_at**	*POLQ*	0.0444	0.5
217535_at	*FAM49B*	0.0331	1.22	**1564190_x_at**	*ZNF519*	0.0166	0.5
226417_at	*RHOB*	0.0433	1.21	**208782_at**	*FSTL1*	0.0393	0.49
221325_at	*KCNK13*	0.0497	1.18	**225450_at**	*AMOTL1*	0.0172	0.48
233344_x_at	*KIAA1875*	0.0259	1.18	**204127_at**	*RFC3*	0.0322	0.48
231158_x_at	*PTBP1*	0.0433	1.18	**210102_at**	*VWA5A*	0.013	0.48
204311_at	*ATP1B2*	0.0172	1.16	**235333_at**	*B4GALT6*	0.0316	0.47
216334_s_at	*CYP2A7P1*	0.0316	1.16	**227554_at**	*MAGI2-AS3*	0.000265	0.47
216352_x_at	*PCDHGA3*	0.0489	1.16	**214620_x_at**	*PAM*	0.000265	0.47
233242_at	*WDR73*	0.0438	1.16	**227542_at**	*SOCS6*	0.0372	0.47
207663_x_at	*GAGE3*	0.0338	1.15	**203129_s_at**	*KIF5C*	< 1e-07	0.46
210498_at	*CLTC*	0.0444	1.13	**218326_s_at**	*LGR4*	0.00927	0.46
208645_s_at	*RPS14*	0.0444	1.13	**218676_s_at**	*PCTP*	0.0174	0.46

200025_s_at	*RPL27*	0.0308	1.12	**212699_at**	*SCAMP5*	0.0255	0.46
242006_at	*LCA5*	0.024	0.9	**204324_s_at**	*GOLIM4*	0.0117	0.44
227526_at	*CDON*	0.0374	0.84	**201063_at**	*RCN1*	0.0424	0.44
1560537_at	*LOC100129662*	0.0444	0.83	**223740_at**	*AGPAT4-IT1*	0.0218	0.43
209897_s_at	*SLIT2*	0.0326	0.83	**215046_at**	*C2orf67*	0.0486	0.43
236551_at	*ZNF311*	0.000114	0.82	**219179_at**	*DACT1*	0.0161	0.43
204455_at	*DST*	0.0268	0.81	**230060_at**	*CDCA7*	0.0317	0.42
220253_s_at	*LRP12*	0.0231	0.8	**201219_at**	*CTBP2*	0.0308	0.42
211298_s_at	*ALB*	0.00664	0.79	**1565786_x_at**	*FLJ45482*	0.00104	0.42
1569352_at	*FNIP2*	0.0308	0.79	**219213_at**	*JAM2*	0.0184	0.42
1556263_s_at	*PWRN1*	0.0322	0.79	**234985_at**	*LDLRAD3*	0.00021	0.42
226863_at	*FAM110C*	0.0308	0.78	**219693_at**	*AGPAT4*	0.00779	0.41
226145_s_at	*FRAS1*	0.0286	0.78	**221606_s_at**	*HMGN5*	0.0402	0.41
1557070_at	*LOC100130275*	0.0406	0.78	**214920_at**	*THSD7A*	0.0368	0.41
1556039_s_at	*GPR173*	0.0172	0.77	**235205_at**	*OXR1*	< 1e-07	0.4
233865_at	*NPAS3*	0.00116	0.77	**205573_s_at**	*SNX7*	0.0199	0.4
226829_at	*AFAP1L2*	0.0338	0.76	**228086_at**	*STK33*	0.0349	0.4
234992_x_at	*ECT2*	0.029	0.76	**225288_at**	*COL27A1*	0.00927	0.39
219882_at	*TTLL7*	0.0338	0.76	**230446_at**	*LOC100506130*	0.0149	0.39
226814_at	*ADAMTS9*	0.0345	0.75	**238605_at**	*NOL4*	0.0393	0.39
241456_at	*FAM78B*	0.00374	0.75	**202446_s_at**	*PLSCR1*	0.0331	0.38
225474_at	*MAGI1*	0.00155	0.75	**1569323_at**	*PTPRG*	0.0228	0.38
208591_s_at	*PDE3B*	0.0272	0.75	**214051_at**	*TMSB15B*	0.0299	0.38
1565149_at	*DYNC2H1*	0.0151	0.74	**215111_s_at**	*TSC22D1*	0.0426	0.37
236112_at	*LOC285548*	0.00332	0.74	**232398_at**	*CCDC150*	0.00188	0.36
244267_at	*SATB1*	0.00473	0.74	**229506_at**	*PPM1L*	0.0298	0.36
237167_at	*KIAA1217*	0.0412	0.73	**205990_s_at**	*WNT5A*	0.0152	0.36
213012_at	*NEDD4*	0.00829	0.73	**225062_at**	*LOC389831*	0.0118	0.35
207437_at	*NOVA1*	0.0353	0.73	**221805_at**	*NEFL*	0.0128	0.34
220014_at	*PRR16*	0.0198	0.73	**226677_at**	*ZNF521*	0.00888	0.34
213325_at	*PVRL3*	0.00786	0.73	**218694_at**	*ARMCX1*	0.000114	0.33
232226_at	*LRRC4C*	0.000336	0.71	**213385_at**	*CHN2*	0.00281	0.33
213558_at	*PCLO*	0.0017	0.71	**235405_at**	*GSTA4*	0.00927	0.33
213283_s_at	*SALL2*	0.0478	0.71	**221538_s_at**	*PLXNA1*	0.0128	0.33
226569_s_at	*CHTF18*	0.0321	0.7	**203875_at**	*SMARCA1*	0.0168	0.33
231738_at	*PCDHB7*	0.0338	0.7	**213110_s_at**	*COL4A5*	< 1e-07	0.32
233209_at	*LOC200609*	0.0372	0.69	**226653_at**	*MARK1*	< 1e-07	0.32
228044_at	*SERP2*	0.0227	0.69	**236337_at**	*SYCP2L*	0.0468	0.32
1569996_at	*ANKRD26P3*	0.0323	0.68	**224403_at**	*FCRL4*	0.00332	0.31
244324_at	*C18orf54*	0.0271	0.68	**212636_at**	*QKI*	0.0112	0.31
211555_s_at	*GUCY1B3*	0.0118	0.68	**203387_s_at**	*TBC1D4*	0.0308	0.31
227088_at	*PDE5A*	0.00138	0.68	**212771_at**	*FAM171A1*	0.0168	0.3
214063_s_at	*TF*	0.00137	0.68	**223627_at**	*MEX3B*	0.00345	0.3
232635_at	*CEP128*	0.0173	0.67	**203000_at**	*STMN2*	0.0086	0.3
205073_at	*CYP2J2*	0.0012	0.67	**203628_at**	*IGF1R*	0.0424	0.29
205201_at	*GLI3*	0.0241	0.67	**210852_s_at**	*AASS*	< 1e-07	0.28
228579_at	*KCNQ3*	0.00173	0.67	**228365_at**	*CPNE8*	< 1e-07	0.27
226225_at	*MCC*	0.00121	0.67	**203680_at**	*PRKAR2B*	0.0168	0.25
211987_at	*TOP2B*	0.0359	0.67	**220231_at**	*C7orf16*	0.00104	0.24

210473_s_at	*GPR125*	0.0218	0.66	**206404_at**	*FGF9*	0.00779	0.24
1556698_a_at	*GPRIN3*	0.0261	0.66	**212192_at**	*KCTD12*	0.0208	0.24
226770_at	*MAGI3*	0.00101	0.66	**217894_at**	*KCTD3*	< 1e-07	0.24
219596_at	*THAP10*	0.0177	0.66	**229331_at**	*SPATA18*	0.000336	0.24
226032_at	*CASP2*	0.0402	0.65	**213273_at**	*ODZ4*	0.000961	0.23
241627_x_at	*ARHGEF40*	0.027	0.64	**219368_at**	*NAP1L2*	< 1e-07	0.22
203692_s_at	*E2F3*	0.0104	0.64	**219855_at**	*NUDT11*	0.00384	0.22
219522_at	*FJX1*	0.000114	0.64	**242912_at**	*POTEM*	< 1e-07	0.22
223488_s_at	*GNB4*	0.00639	0.63	**225731_at**	*ANKRD50*	< 1e-07	0.21
1559826_a_at	*LOC401074*	0.000114	0.63	**203139_at**	*DAPK1*	0.0141	0.2
209124_at	*MYD88*	0.0437	0.63	**226184_at**	*FMNL2*	0.0218	0.19
220520_s_at	*NUP62CL*	0.00927	0.63	**226084_at**	*MAP1B*	0.0194	0.19
232803_at	*FLJ31958*	0.0338	0.62	**223313_s_at**	*MAGED4*	0.012	0.17
219338_s_at	*LRRC49*	0.000497	0.62	**226189_at**	*ITGB8*	0.00315	0.16
228584_at	*SGCB*	0.000114	0.62	**225745_at**	*LRP6*	0.00195	0.16
216195_at	*ANK2*	0.0496	0.61	**229963_at**	*BEX5*	0.000265	0.15
205848_at	*GAS2*	0.0407	0.61	**205110_s_at**	*FGF13*	< 1e-07	0.15
225158_at	*GFM1*	0.0352	0.61	**242136_x_at**	*MGC70870*	0.0113	0.15
219287_at	*KCNMB4*	0.0118	0.61	**219355_at**	*CXorf57*	0.0012	0.14
215692_s_at	*MPPED2*	0.00575	0.61	**204749_at**	*NAP1L3*	< 1e-07	0.14
206825_at	*OXTR*	0.00296	0.61	**228494_at**	*PPP1R9A*	0.00138	0.14
213119_at	*SLC36A1*	0.0209	0.61	**209732_at**	*CLEC2B*	0.0327	0.13
238067_at	*TBC1D8B*	0.00101	0.61	**217975_at**	*WBP5*	< 1e-07	0.13
235775_at	*TMTC2*	0.0172	0.61	**215017_s_at**	*FNBP1L*	0.00781	0.11
226492_at	*SEMA6D*	0.00543	0.59	**217963_s_at**	*NGFRAP1*	< 1e-07	0.081
204451_at	*FZD1*	0.00631	0.58	**213194_at**	*ROBO1*	< 1e-07	0.017

Table S13. Primers used for Sanger sequencing in the validation analysis.

Gene	Primer	Exon	Sequence (5'-3')
BIRC3	F	9	CTGAAGAAGCAAACTGCCTTT
	R	9	AAGGAAACCAAATTAGGATAAAAGTT
B2M	F	1	CTGGCTTGGAGACAGGTGAC
	R	1	AGATCCAGCCCTGGACTAGC
	F	2	GGGAGAAATCGATGACCAAA
	R	2	CATTCCCTGACAATCCCAAT
	F	3	TGGGTAGGAACAGCAGCCTA
	R	3	CAGTTCCTTTGCCCTCTCTG
DBC1*	F	8	TTTCGCAGTAGGGTAGGTAGCC
	F'	8	TTTCGCAGTAGGGTAGGTAGCT
	R	8	CGAGCAGTTCATCAGCTTTG
MEF2B	F	1	CCCCCTGCTAGGAATGTCTT
	R	1	TCCCCATCATCTTCCTCTCA
	F	2	AGTCCCTGGGCTCTGAGAA
	R	2	ACCAGCTCAGCCAGAAAGAA
	F	3	TGAAGGAAGGAACTGTTTGC
	R	3	GCCATGCCTGCATTCCTC
	F	4-5	CCTCACTCACGGAGGTGTTT
	R	4-5	GTAGAGCTGGGCCCCTGA
	F	6-7	GAGGACCCTGGGAAAGGAG
	R	6-7	GTTTCCCCTTCACCCTCTCT
	F	8	GCGCGTTTTATTTGTGGATA
	R	8	GATGGGCAGCTATTTTGAGG
NOTCH1	F	26	ACTGCAAGGACCACTTCAGC
	R	26	GTCCATGGGGTCCAGCTC
	F	34-A	CGGAGGAGGTTGTACTGCTG
	R	34-A	GGACGGAGACTGCTGGAAC
	F	34-B	ATGGCTACCTGTCAGACGTG
	R	34-B	TCTCCTGGGGCAGAATAGTG
	F	34-C	GAGCTTCCTGAGTGGAGAGC
	R	34-C	CCTGGCTCTCAGAACTTGCT
NOTCH2	F	26	TTTGCCTGTTCTCTGCTTCC
	R	26	GCCTTGAAGTTCAGAAACCAA
	F	27	TTACCCCCATCTCTCCTCCT
	R	27	TTTCCCCTTTACACCAGTGC
	F	34-A	AGGCACAGCCTATCTGTGGT
	R	34-A	GGCATGGTACTCTTGGCACT
	F	34-B	CCCAATGGGCAAGAAGTCTA
	R	34-B	CACAATGTGGTGGTGGGATA
	F	34-C	CATGAAATGCAGCCTTTGG
	R	34-C	GGCCATTTCTGGAATCTGGT
	F	34-D	AAGGCAGTATTGCCCAACC
	R	34-D	TCATTTCTCTCCCGGATGAC
TLR2	F	1	TGTGAAAATCACCGATGAAAG
	R	1	TGTTGTGAAAGTAAACAAGGAACC
TP53	F	4	TGCTCTTTTCACCCATCTAC
	R	4	ATACGGCCAGGCATTGAAGT
	F	5-6	TGTTCACTTGTGCCCTGACT
	R	5-6	TTAACCCCTCCTCCCAGAGA
	F	8-9	TTGGGAGTAGATGGAGCCT
	R	8-9	AGTGTTAGACTGGAAACTTT
	F	10	CAATTGTAACTTGAACCATC
	R	10	GGATGAGAATGGAATCCTAT
	F	11	AGACCCTCTCACTCATGTGA
	R	11	TGACGCACACCTATTGCAAG
WHSC1	F	18	GTGTGGTGCCCGTTCTAAGT
	R	18	CACAGGGCAAAGTCCAGTTC
	F	19	CATGCGATTGCTAACACTTGA
	R	19	TCAAACCAAAAGAGACTCCACA

F: forward; R: reverse

*Specific primers with the mutation allele or wild type allele in the forward primer, only used to check the two *cis*-mutations in the same case (M014).

SUPPLEMENTARY REFERENCES

1. Swerdlow, S., Campo, E., Harris, N., Jaffe, E., Pileri, S., Stein, H., Thiele, J., & Vardiman, J (Eds.). (2008) *WHO Classification of Tumours of Haematopoietic and Lymphoid Tissues*. IARC: Lyon 2008.

2. Hudson TJ et al. (2010) International network of cancer genome projects. *Nature* 464(7291):993-998.

3. Puente XS et al. (2011) Whole-genome sequencing identifies recurrent mutations in chronic lymphocytic leukaemia. *Nature* 475(7354):101-105.

4. Quesada V et al. (2012) Exome sequencing identifies recurrent mutations of the splicing factor SF3B1 gene in chronic lymphocytic leukemia. *Nat Genet* 44(1):47-52.

5. Navarro A et al. (2012) Molecular subsets of mantle cell lymphoma defined by the IGHV mutational status and SOX11 expression have distinct biologic and clinical features. *Cancer Res* 72(20):5307-5316.

6. Nik-Zainal S et al. (2012) Mutational processes molding the genomes of 21 breast cancers. *Cell* 149(5):979-993.

7. Hadzidimitriou A et al. (2011) Is there a role for antigen selection in mantle cell lymphoma? Immunogenetic support from a series of 807 cases. *Blood* 118(11):3088-3095.

8. Rausch T et al. (2012) Genome sequencing of pediatric medulloblastoma links catastrophic DNA rearrangements with TP53 mutations. *Cell* 148(1-2):59-71.

9. Valdes-Mas R, Bea S, Puente DA, Lopez-Otin C, Puente XS (2012) Estimation of copy number alterations from exome sequencing data. *PLoS One* 7(12):e51422.

10. Greiner TC et al. (2006) Mutation and genomic deletion status of ataxia telangiectasia mutated (ATM) and p53 confer specific gene expression profiles in mantle cell lymphoma. *Proc Natl Acad Sci U S A* 103(7):2352-2357.

11. Fang NY et al. (2003) Oligonucleotide microarrays demonstrate the highest frequency of ATM mutations in the mantle cell subtype of lymphoma. *Proc Natl Acad Sci U S A* 100(9):5372-5377.

12. Bullrich F et al. (1999) ATM mutations in B-cell chronic lymphocytic leukemia. *Cancer Res* 59(1):24-27.

13. Schaffner C, Stilgenbauer S, Rappold GA, Dohner H, Lichter P (1999) Somatic ATM mutations indicate a pathogenic role of ATM in B-cell chronic lymphocytic leukemia. *Blood* 94(2):748-753.

14. Stankovic T et al. (1999) Inactivation of ataxia telangiectasia mutated gene in B-cell chronic lymphocytic leukaemia. *Lancet* 353(9146):26-29.

15. Austen B et al. (2005) Mutations in the ATM gene lead to impaired overall and treatment-free survival that is independent of IGVH mutation status in patients with B-CLL. *Blood* 106(9):3175-3182.

16. Guarini A et al. (2012) ATM gene alterations in chronic lymphocytic leukemia patients induce a distinct gene expression profile and predict disease progression. *Haematologica* 97(1):47-55.

17. Mansouri L et al. (2012) Next generation RNA-sequencing in prognostic subsets of chronic lymphocytic leukemia. *Am J Hematol* 87(7):737-740.

18. Ouillette P et al. (2012) Incidence and clinical implications of ATM aberrations in chronic lymphocytic leukemia. *Genes Chromosomes Cancer* 51(12):1125-1132.

19. Skowronska A et al. (2012) Biallelic ATM inactivation significantly reduces survival in patients treated on the United Kingdom Leukemia Research Fund Chronic Lymphocytic Leukemia 4 trial. *J Clin Oncol* 30(36):4524-4532.

20. Kridel R et al. (2012) Whole transcriptome sequencing reveals recurrent NOTCH1 mutations in mantle cell lymphoma. *Blood* 119(9):1963-1971.

21. Shaffer AL et al. (2006) A library of gene expression signatures to illuminate normal and pathological lymphoid biology. *Immunol Rev* 210(1):67-85.

22. Su AI et al. (2004) A gene atlas of the mouse and human protein-encoding transcriptomes. *Proc Natl Acad Sci U S A* 101(16):6062-6067.

23. Cho RJ et al. (2001) Transcriptional regulation and function during the human cell cycle. *Nat Genet* 27(1):48-54.

24. Zhan F et al. (2006) The molecular classification of multiple myeloma. *Blood* 108(6):2020-2028.

25. Martinez-Garcia E et al. (2011) The MMSET histone methyl transferase switches global histone methylation and alters gene expression in t(4;14) multiple myeloma cells. *Blood* 117(1):211-220.

26. Lohr JG et al. (2012) Discovery and prioritization of somatic mutations in diffuse large B-cell lymphoma (DLBCL) by whole-exome sequencing. *Proc Natl Acad Sci U S A* 109(10):3879-3884.

27. Pasqualucci L et al. (2011) Analysis of the coding genome of diffuse large B-cell lymphoma. *Nat Genet* 43(9):830-837.

28. Green MR et al. (2013) Hierarchy in somatic mutations arising during genomic evolution and progression of follicular lymphoma. *Blood* 121(9):1604-1611.

29. Chapman MA et al. (2011) Initial genome sequencing and analysis of multiple myeloma. *Nature* 471(7339):467-472.

30. Morin RD et al. (2011) Frequent mutation of histone-modifying genes in non-Hodgkin lymphoma. *Nature* 476(7360):298-303.

31. Zhang J et al. (2013) Genetic heterogeneity of diffuse large B-cell lymphoma. *Proc Natl Acad Sci U S A* 110(4):1398-1403.

32. Sharma VM et al. (2006) Notch1 contributes to mouse T-cell leukemia by directly inducing the expression of c-myc. *Mol Cell Biol* 26(21):8022-8031.

33. Palomero T et al. (2006) NOTCH1 directly regulates c-MYC and activates a feed-forward-loop transcriptional network promoting leukemic cell growth. *Proc Natl Acad Sci U S A* 103(48):18261-18266.

34. Weng AP et al. (2006) c-Myc is an important direct target of Notch1 in T-cell acute lymphoblastic leukemia/lymphoma. *Genes Dev* 20(15):2096-2109.

35. Weng AP et al. (2003) Growth suppression of pre-T acute lymphoblastic leukemia cells by inhibition of notch signaling. *Mol Cell Biol* 23(2):655-664.

36. Rossi D et al. (2012) The coding genome of splenic marginal zone lymphoma: activation of NOTCH2 and other pathways regulating marginal zone development. *J Exp Med* 209(9):1537-1551.

37. Fabbri G et al. (2011) Analysis of the chronic lymphocytic leukemia coding genome: role of NOTCH1 mutational activation. *J Exp Med* 208(7):1389-1401.

38. Villamor N et al. (2012) NOTCH1 mutations identify a genetic subgroup of chronic lymphocytic leukemia patients with high risk of transformation and poor outcome. *Leukemia* 27(5):1100-1106.